Can we globally optimize cross-validation loss? Quasiconvexity in ridge regression

William T. Stephenson[*]
MIT
wtstephe@mit.edu

Zachary Frangella
Cornell
zjf4@cornell.edu

Madeleine Udell
Cornell
udell@cornell.edu

Tamara Broderick
MIT
tbroderick@mit.edu

Abstract

Models like LASSO and ridge regression are extensively used in practice due to their interpretability, ease of use, and strong theoretical guarantees. Cross-validation (CV) is widely used for hyperparameter tuning in these models, but do practical optimization methods minimize the true out-of-sample loss? A recent line of research promises to show that the optimum of the CV loss matches the optimum of the out-of-sample loss (possibly after simple corrections). It remains to show how tractable it is to minimize the CV loss. In the present paper, we show that, in the case of ridge regression, the CV loss may fail to be quasiconvex and thus may have multiple local optima. We can guarantee that the CV loss is quasiconvex in at least one case: when the spectrum of the covariate matrix is nearly flat and the noise in the observed responses is not too high. More generally, we show that quasiconvexity status is independent of many properties of the observed data (response norm, covariate-matrix right singular vectors, and singular-value scaling) and has a complex dependence on the few that remain. We empirically confirm our theory using simulated experiments.

1 Introduction

Linear models, including LASSO and ridge regression, are widely used for data analysis across diverse applied disciplines. Linear models are often preferred since they are straightforward to apply in various senses. In particular, (1) their parameters are readily interpretable. (2) They have strong theoretical guarantees on quality. And (3) standard optimization tools are often assumed to find useful parameter and hyperparameter values. Despite their seeming simplicity, though, mysteries remain about the quality of inference in linear models. Consider cross-validation (CV) [Stone, 1974, Allen, 1974], the de facto standard for hyperparameter selection across machine learning methods [Musgrave et al., 2020]. CV is an easy-to-evaluate proxy for the true out-of-sample loss. Is it a good proxy? [Homrighausen and McDonald, 2014, 2013, Chetverikov et al., 2020, Hastie et al., 2020, Patil et al., 2021] give conditions under which the global minimum of the CV loss (possibly with some mild corrections) matches the optimum of the out-of-sample loss in LASSO and ridge regression. To complete the picture, we must understand whether standard methods for minimizing the CV loss find a global minimum.

It would be easy to find a unique minimum of the CV loss if the CV loss were convex. Alas (though perhaps unsurprisingly), we show below that in essentially every case of interest the CV loss is not convex. Indeed, the usual introductory cartoon of CV loss (left panel of Fig. 1; see also Fig. 5.9 of Hastie et al. [2017] or Fig. 1 of Rad and Maleki [2020]) is not convex. But the cartoon CV loss still exhibits a single global minimum and would be easy to globally minimize with popular approaches like gradient-based methods [Do et al., 2007, Maclaurin et al., 2015, Pedregosa, 2016, Lorraine et al., 2020] or grid search [Bergstra and Bengio, 2012, Pedregosa et al., 2011, Hsu et al., 2003]. Indeed, a

---

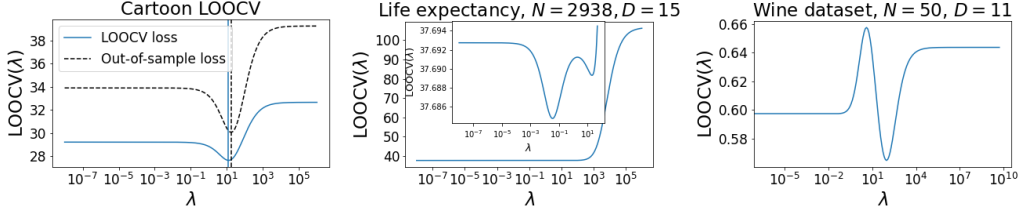[*]Alternate email: wtstephe@gmail.com

Figure 1: (*Left*): Idealized illustration of the leave-one-out CV loss $\mathcal{L}$ (blue) and the true out-of-sample loss (black). The minimizer of each curve is marked with a vertical line of the corresponding color. (*Center*): CV loss for a life-expectancy prediction problem after some standard data pre-processing (Condition 1 of Section 2). (*Right*): CV loss for wine-quality prediction problem on a subset of $N = 50$ data points after standard data pre-processing (Condition 1 of Section 2).

more plausible possibility (which holds for the typical cartoon CV loss) is that the CV loss might be *quasiconvex*; i.e. its level sets are convex. The benefit of quasiconvexity is that, in one dimension, any local optimum is a global optimum.

Unfortunately, this cartoon need not hold in general, even in simple models like ℓ_2-regularized linear regression (i.e. ridge regression). Consider minimizing leave-one-out CV (LOOCV) loss as a function of the ridge regularization parameter; we denote this loss by $\mathcal{L}$. Wilson et al. [2020, Fig. 1] detail a simulated example in which $\mathcal{L}$ can be non-quasiconvex. We first demonstrate that $\mathcal{L}$ can be non-quasiconvex in real-data examples; see the middle and right panel of Fig. 1, which we describe in detail in Section 3. We next characterize which aspects of the covariate matrix and observed responses affect quasiconvexity. We prove that the norm of the responses, the scale of the singular values of the covariate matrix, and the right singular vectors of the covariate matrix all have no effect on the quasiconvexity of $\mathcal{L}$. While this result places substantial constraints on what drives the quasiconvexity of $\mathcal{L}$, we show that the quasiconvexity of $\mathcal{L}$ is unfortunately still a complex function of the remaining quantities. Our third contribution is to prove conditions under which $\mathcal{L}$ is guaranteed to be quasiconvex. In particular, we show that if (1) the covariate matrix has a singular value spectrum sufficiently close to uniform, (2) the least-squares estimator fits the training data sufficiently well, and (3) the left singular vectors of the covariate matrix are sufficiently regular, then $\mathcal{L}$ is guaranteed to be quasiconvex. While the conditions of our theory are deterministic, we show that they have natural probabilistic interpretations; as a corollary to our theory, we demonstrate that many of our conditions are satisfied either empirically or theoretically by well-specified linear regression problems with i.i.d. sub-Gaussian covariates and moderate signal-to-noise ratios. Through empirical studies, we validate the conclusions of our theory and the necessity of our assumptions.

2   Setup and notation

For $n \in \{1, \ldots, N\}$, we observe covariates $x_n \in \mathbb{R}^D$ and responses $y_n \in \mathbb{R}$. We are interested in learning a linear model between the covariates and responses, $\langle x_n, \theta \rangle \approx y_n$, for some parameter $\theta \in \mathbb{R}^D$. In ridge regression, i.e. ℓ_2-regularized linear regression, we take some $\lambda > 0$ and estimate:

$$\hat{\theta}(\lambda) := \arg\min_{\theta \in \mathbb{R}^D} \sum_{n=1}^N (\langle x_n, \theta \rangle - y_n)^2 + \frac{\lambda}{2} \|\theta\|_2^2 . \tag{1}$$

The regularization parameter λ is typically chosen by minimizing the cross-validation (CV) loss. Here we study the leave-one-out CV (LOOCV) loss:

$$\mathcal{L}(\lambda) := \sum_{n=1}^N \left(\langle x_n, \hat{\theta}^{\backslash n}(\lambda) \rangle - y_n \right)^2 , \tag{2}$$

where $\hat{\theta}^{\backslash n}(\lambda)$ is the solution to Eq. (1) with the nth datapoint left out.

Let the covariate matrix $X \in \mathbb{R}^{N \times D}$ be the matrix with rows x_n, and let the vector $Y \in \mathbb{R}^N$ be the vector with entries y_n. We consider the low to modest-dimensional case where $D < N$ and assume the covariate matrix X is full-rank. We further assume X and Y have undergone standard data pre-processing, as described next.

2

Condition 1. *Y is zero-mean, and X has zero-mean, unit variance columns. Equivalently, where $\mathbf{1} \in \mathbb{R}^N$ is the vector of all ones, $\mathbf{1}^T Y = 0$ and $X^T \mathbf{1} = \mathbf{0} \in \mathbb{R}^D$ and for all $d = 1, \ldots, D$, $\sum_{n=1}^{N} x_{nd}^2 = N$.*

Preprocessing X and Y to satisfy Condition 1 represents standard best practice for ridge regression. First, using an unregularized bias parameter in Eq. (1) and setting Y to be zero-mean are equivalent; we choose to make Y zero-mean, as it simplifies our analysis below. The conditions on the covariate matrix X are important to ensure the use of ℓ_2-regularization is sensible. In particular, Eq. (1) penalizes all coordinates of θ equally. If e.g. some columns of X are measured in different scales or are centered differently, this uniform penalty will be inappropriate.

3 LOOCV loss is typically not convex and need not be quasiconvex

If the LOOCV loss $\mathcal{L}$ were convex or quasiconvex in λ, then any local minimum of $\mathcal{L}$ would be a global minimum, and we could trust gradient-based optimization methods or grid search methods to return a value near a global minimum. We next see that unfortunately $\mathcal{L}$ is typically not convex and is often not even quasiconvex. First we show that, in essentially all cases of interest, $\mathcal{L}$ is *not* convex.

Proposition 1. *If $\lambda = \infty$ is not a minimum of $\mathcal{L}$, then $\mathcal{L}$ is not a convex function.*

Proof. For the sake of contradiction, assume $\mathcal{L}$ is convex and $\lambda = \infty$ is not a minimum of $\mathcal{L}$. This implies that there is some maximal $\lambda^* < \infty$ such that $\mathcal{L}'(\lambda^*) = 0$. Let $\delta := \mathcal{L}'(\lambda^* + 1)$. By convexity, $\mathcal{L}'' \geq 0$, so we know that $\delta > 0$ and that for $\lambda \geq \lambda^* + 1$, we have $\mathcal{L}'(\lambda) \geq \delta$. Thus for $\lambda \geq \lambda^* + 1$, we have $\mathcal{L}(\lambda) \geq \delta(\lambda - \lambda^* - 1)$. So $\lim_{\lambda \to \infty} \mathcal{L}(\lambda) = \infty$. However, inspection of $\mathcal{L}$ shows $\lim_{\lambda \to \infty} \mathcal{L}(\lambda) = \sum_{n=1}^{N} y_n^2 < \infty$, which is a contradiction. $\square$

We say that the result covers essentially all cases of interest: if $\mathcal{L}$ continues to decrease as $\lambda \to \infty$, then there is so little signal in the data that the zero model $\theta = \mathbf{0} \in \mathbb{R}^D$ is the optimal predictor according to LOOCV.

Although $\mathcal{L}$ is generally not convex, $\mathcal{L}(\lambda)$ might still be easy to optimize if it satisfies an appropriate generalized notion of convexity. To that end, we recall the definition of quasiconvexity.

Definition 1. *A function $f : \mathbb{R}^p \to \mathbb{R}$ is* quasiconvex *if its level sets are convex.*

In one dimension (i.e. $p = 1$ in Definition 1), quasiconvexity guarantees that any local optimum is a global optimum, just as convexity does. This property is often the key consideration in practical optimization algorithms. Moreover, it is not unreasonable to hope that the CV loss is quasiconvex: typical illustrations of the CV loss are not convex but are quasiconvex; see e.g. Hastie et al. [2015, Fig. 5.9], Rad and Maleki [2020, Fig. 1], or the left panel of Fig. 1. Illustrations of the out-of-sample loss are also typically quasiconvex; see e.g. Fig. 3.6 of Bishop [2006].

Unfortunately, we next demonstrate that the CV loss derived from real data analysis problems can be non-quasiconvex. Our first dataset contains $N = 2{,}938$ observations of life expectancy, along with $D = 20$ covariates such as country of origin or alcohol use; see Appendix A for a full description. In this case, after pre-processing according to Condition 1, $\mathcal{L}$ for the full dataset is quasiconvex. But now consider some additional standard data pre-processing. Practitioners often perform principal component regression (PCR) with the aim of reducing noise in the estimated θ. That is, they take the singular value decomposition of $X = USV$ and produce an $N \times R$ dimensional covariate matrix X' by retaining just the top R singular values of X: $X' = U_{.,:R} S_{:R}$. With this pre-processing, the resulting LOOCV curve $\mathcal{L}$ is non-quasiconvex for many values of R; in the center panel of Fig. 1 we show one example for $R = 15$.

Our second dataset consists of recorded wine quality of $N = 1{,}599$ red wines. The goal is to predict wine quality from $D = 11$ observed covariates relating to the chemical properties of each wine; see Appendix A for a full description. We find that subsets of this dataset often exhibit non-quasiconvex $\mathcal{L}$. In the right panel of Fig. 1, we show $\mathcal{L}$ for a subset of size $N = 50$. We see that this plot contains at least two local optima, with substantially different values of λ and substantially different values of the loss. A gradient-based algorithm initialized sufficiently far to the left would not find the global optimum, and grid search without sufficiently large values would not find the global optimum.

Now we know that $\mathcal{L}$ can be non-quasiconvex for real data. Given the difficulty of optimizing a function with several local minima, we next seek to understand *when* $\mathcal{L}$ is quasiconvex or not.

4 What does the quasiconvexity of $\mathcal{L}$ depend on?

We have seen that $\mathcal{L}$ can be quasiconvex or non-quasiconvex, depending on the data at hand. If we could determine the quasiconvexity of $\mathcal{L}$ from the data, we might better understand how to efficiently tune hyperparameters from the CV loss. In what follows, we start by showing that the quasiconvexity of $\mathcal{L}$ is, in fact, independent of many aspects of the data (Proposition 2). We will see, however, that the dependence of quasiconvexity on the remaining aspects (though they are few) is complex.

A linear regression problem has a number of moving parts. The response vector Y may be an arbitrary vector in $\mathbb{R}^N$, and the covariate matrix X can be written in terms of its singular values and left and right singular vectors. More precisely, let $X = U \operatorname{diag}(S) V^T$ be the singular value decomposition of the covariate matrix X, where $U \in \mathbb{R}^{N \times D}$ is an $N \times D$ matrix with orthonormal columns, $S \in \mathbb{R}^D$ is a vector with positive entries, and $V \in \mathbb{R}^{D \times D}$ is an orthonormal matrix. Note we use the "compact" singular value decomposition, where U is a $N \times D$ matrix, rather than a full $N \times N$ matrix. With this notation in hand, we can identify aspects of the problem that do not contribute to quasiconvexity in the following result, which is proved in Appendix B.

Proposition 2. *The quasiconvexity of $\mathcal{L}$ is independent of*

1. *the matrix of right singular vectors, V,*

2. *the norm of the responses, $\|Y\|_2$, and*

3. *the scaling of the singular values (i.e. changing S into S/c for $c \in \mathbb{R}_{>0}$),*

in the sense that altering any of these quantities does not change whether or not $\mathcal{L}$ is quasiconvex.

Remark 1. *Assume Condition 1 holds. Then by Proposition 2, without loss of generality we may (and do) assume that $V = I_D$ and that Y is a vector on the unit $(N-1)$-sphere.*

Recall X has zero-mean columns by pre-processing the data (Condition 1). By Proposition 2, we assume without loss of generality $V = I_D$. Thus, the columns of X have zero mean when $U^T \mathbf{1} = 0$, where $\mathbf{1} \in \mathbb{R}^N$ is the vector of all ones. Also, while Remark 1 notes that we can consider Y to be on the unit $(N-1)$-sphere, note that the condition $\mathbf{1}^T Y = 0$ from Condition 1 allows us to further constrain Y to be parameterized by a vector on the unit $(N-2)$-sphere. Hence the quasiconvexity of $\mathcal{L}$ depends on three quantities: (1) the matrix of left singular vectors, U, an orthonormal matrix with $\mathbf{1} \in \mathbb{R}^N$ in its left null-space, (2) the (normalized) vector Y which sits on the unit $(N-2)$-sphere, and (3) the (normalized) singular values.

Now that we know the quasiconvexity of $\mathcal{L}$ depends on only three quantities, we might hope that quasiconvexity would be a simple function of the three. To investigate this dependence, we consider the case of $N = 3$ and $D = 2$, since this case is particularly easy to visualize. To see why it is easy to visualize, first note that Y is a three-dimensional vector; thus by our discussion above, we can parameterize Y by a vector on the unit circle (i.e. a scalar between 0 and 2π). Second, note that the matrix of left singular vectors U is parameterized by two orthonormal vectors, $U_{\cdot 1}$ and $U_{\cdot 2}$, each on the unit 2-sphere. As both vectors must be orthogonal to $\mathbf{1} \in \mathbb{R}^3$, we can parameterize $U_{\cdot 1}$ and $U_{\cdot 2}$ by two orthonormal vectors on the unit circle. We parametrize $U_{\cdot 1}$ by a scalar that determines $U_{\cdot 2}$ up to a rotation of $U_{\cdot 2}$ by π. We fix a rotation for $U_{\cdot 2}$ relative to $U_{\cdot 1}$ so that, for fixed singular values S, the quasiconvexity of $\mathcal{L}$ is parameterized by two scalars.

Fig. 2 is the resulting visualization. Precisely, to make Fig. 2, we fix an orientation between $U_{\cdot 1}$ and $U_{\cdot 2}$: here, a rotation of $\pi/2$ on the unit circle. We create a uniform grid over the unit circles for $U_{\cdot 1}$ and Y. Fig. 2 visualizes the *severity* of non-quasiconvexity of $\mathcal{L}$ as we move over this grid for three different settings of the singular values. To define the severity of non-quasiconvexity, let λ_{worst}, λ^*, and $\lambda_{\text{worst-min}}$ correspond to the λ maximizing $\mathcal{L}$, the λ minimizing $\mathcal{L}$, and the λ corresponding to the local minimum with largest $\mathcal{L}$, respectively. We then compute

$$\text{severity} := \frac{\mathcal{L}(\lambda_{\text{worst-min}}) - \mathcal{L}(\lambda^*)}{\mathcal{L}(\lambda_{\text{worst}}) - \mathcal{L}(\lambda^*)} \tag{3}$$
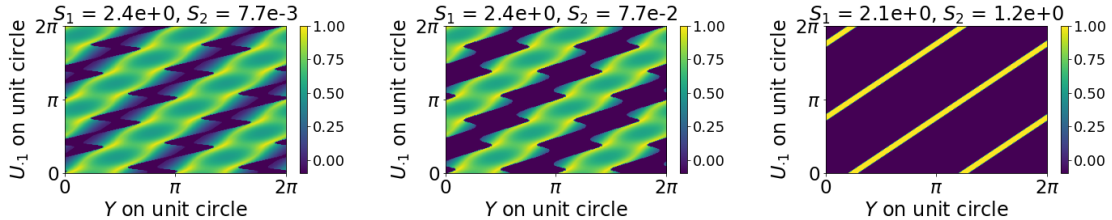
4

Figure 2: How does quasiconvexity depend on Y and U, for data with $N = 3$ and $D = 2$? The left, center, and right panels each correspond to a different setting of the singular values S. We divide the unit circle for each of U and Y into 225 equally spaced points. We examine the severity of non-quasiconvexity in $\mathcal{L}$ over this 225×225 grid. Each grid point is colored by Eq. (3), where dark purple corresponds to quasiconvexity (no local minima).

If the severity is near 1, then finding the worst local minimum is nearly as bad as selecting the worst possible λ. In Fig. 2 we color pixels according to this measure of severity and do in fact see values near 1. We see that, in general, U, Y, and S have a complicated interaction to determine the quasiconvexity of $\mathcal{L}$. The values of Y that produce quasiconvexity depend on U. No setting of Y or U guarantees quasiconvexity.

Fig. 2 demonstrates the poor performance of a hypothetical optimizer that always finds the worst local minimum. In Appendix C, we show that poor performance is not just hypothetical; in particular, the most commonly used methods for optimizing $\mathcal{L}$ – grid search and gradient descent – encounter difficulties due to non-quasiconvexity. Issues due to non-quasiconvexity are also not specific to measuring performance in terms of $\mathcal{L}$ nor to optimizing the LOOCV loss. In Appendix C, we show that the K-fold CV loss also suffers from non-quasiconvexity and that computing Eq. (3) with the test loss instead of $\mathcal{L}$ also exhibits issues due to non-quasiconvexity.

Despite the complexity of Fig. 2, one trend does seem clear: as the singular values become more similar (moving from left to right in the panels of Fig. 2), the fraction of Y values and U values that correspond to quasiconvexity (dark purple regions) grows. Based on this behavior, one might conjecture that a sufficiently uniform spectrum of the covariate matrix could guarantee the quasiconvexity of $\mathcal{L}$.

5 Quasiconvexity of $\mathcal{L}$ with a nearly uniform spectrum S

We now build on the conjecture of the previous section to show that we can, in fact, guarantee quasiconvexity in certain cases. In particular, we will show conditions under which a sufficiently uniform spectrum S of the covariate matrix X guarantees that $\mathcal{L}$ is quasiconvex.

One might hope that for large N, eventually any Y or U would yield quasiconvexity. However, even when S is exactly uniform, our experiments in Section 6 show that we cannot expect such a statement. Rather, we will devise conditions on Y and U to avoid "extreme" settings for either quantity. With these conditions, our main theorem will show that a sufficiently flat spectrum S does indeed guarantee quasiconvexity of $\mathcal{L}$. When our theorem applies, we can safely terminate an optimization procedure at the first local minimum of $\mathcal{L}$ that we discover.

We first establish notation and then state our assumptions.

Definition 2. *Let* $\hat{\theta} := \left(X^T X \right)^{-1} X^T Y$ *be the least-squares estimate. Define the least-squares residuals* $\hat{E} := Y - X\hat{\theta}$. *Let* $\hat{\varepsilon}_n$ *be the* nth *entry of* $\hat{E}$.

Note that $\hat{\theta}$ is well-defined since we have assumed that $D < N$ and that X is full-rank. For the tractability of our theory, all of our assumptions and conclusions will be asymptotic in N; in particular, our assumptions will use big-O and little-o statements, which are to be taken with respect to N growing large. In our discussion of these assumptions, we assume that D is fixed. There is nothing in our proofs or assumptions that requires D to be fixed; however the validity of our assumptions is not clear if D grows with N, so we do not consider this case here. Since LOOCV is useful precisely for

finite N, we are careful to show in our experiments (Section 6) that these asymptotics take hold for small N.

Our first assumption concerns the magnitude of the residuals $\hat{E}$.

Assumption 1. $(1/N) \sum_{n=1}^{N} \hat{\varepsilon}_n^2$ *is* $O(1)$ *(i.e. it does not grow with N).*

This assumption is fairly lax. For example, suppose our linear model is well-specified. In particular, suppose there exists some $\theta^* \in \mathbb{R}^D$ such that $y_n = \langle x_n, \theta^* \rangle + \varepsilon_n$ where the ε_n are i.i.d. $\mathcal{N}(0, \sigma^2)$ for some $\sigma > 0$. Stack the ε_n into a vector $E \in \mathbb{R}^N$. Then $\|\hat{E}\|^2 = \|(I_N - UU^T)E\|^2 < \|E\|^2$. Since $(1/N)\|E\|^2$ is $O(1)$ with high probability, it follows that Assumption 1 holds with high probability in this well-specified linear model. We emphasize that Assumption 1 depends on the residuals of the least squares estimate, not (directly) on the noise in the observations.

Our next assumption governs the size of the least squares estimate $\hat{\theta}$.

Assumption 2. $\|\hat{\theta}\|$ *is* $O(1)$ *(i.e. it does not grow with N).*

Again, this is a lax assumption. For example, given any statistical model for which $\hat{\theta}$ is a consistent estimator for some quantity, Assumption 2 holds.

Our next assumption constrains the uniformity of the left-singular value matrix U with rows $u_n \in \mathbb{R}^D$.

Assumption 3. *We have* $\max_n \|u_n\|^2 := \|u_{\max}\|^2 = O(N^{-p})$ *for some $p > 1/2$.*

Assumption 3 is an assumption about the coherence of the U matrix, a quantity of importance in compressed sensing and matrix completion [Candés and Recht, 2009]. In particular, Assumption 3 requires that the coherence of U decay sufficiently fast as a function of N. Suppose we remove the condition that U have zero-mean columns (see Condition 1 and the discussion after Remark 1) and assume a uniform distribution over valid U (i.e. matrices with orthonormal columns); then Assumption 3 is known to hold with high probability for any $p \in (1/2, 1)$ [Candés and Recht, 2009, Lemma 2.2].

There do exist matrices U with orthonormal zero-mean columns that do not satisfy Assumption 3. For instance, take some small N_0 (say $N_0 = 5$) and a valid U' for this N_0. Then, for $N > N_0$, form U by appending $\mathbf{0} \in \mathbb{R}^{(N-N_0) \times D}$ to the bottom of U'. This construction yields an $N \times D$ matrix U with orthonormal and zero-mean columns for which $\|u_{\max}\|^2$ is constant as N grows. Still, in our experiments in Section 6 and Appendix D, we confirm that, for a uniform distribution over orthonormal U with zero-mean columns, Assumption 3 holds with high probability.

Our final assumption is a technical assumption relating $\|u_n\|^2$, $\hat{\varepsilon}_n$, and $\hat{\theta}$.

Assumption 4. *The following quantity is positive and $\Theta(1)$ (i.e. is bounded away from zero and does not grow with N):* $\|\hat{\theta}\|^2 - \sum_{n=1}^{N} \|u_n\|^2 \left(\langle u_n, \hat{\theta} \rangle^2 + 2\hat{\varepsilon}_n^2 \right)$

Roughly, this assumptions means that the largest $\|u_n\|^2$ and $\hat{\varepsilon}_n^2$ values do not occur for the same values of n. To see this relation, note that Assumption 3 implies $\|\hat{\theta}\|^2 - \sum_n \|u_n\|^2 \langle u_n, \hat{\theta} \rangle^2 \geq (1 - O(N^{-p}))\|\hat{\theta}\|^2$. If we assume that $\|\hat{\theta}\|^2 = \Theta(1)$ (i.e. Assumption 2 holds and $\hat{\theta}$ does not converge to $\mathbf{0} \in \mathbb{R}^D$), then we find $\|\hat{\theta}\|^2 - \sum_n \|u_n\|^2 \langle u_n, \hat{\theta} \rangle^2 = \Theta(1)$. So, we need only that $\sum_n \|u_n\|^2 \hat{\varepsilon}_n^2 = o(1)$ for Assumption 4 to hold; e.g. we need that the largest values of $\|u_n\|^2$ and the largest values of $\hat{\varepsilon}_n^2$ typically do not occur for the same values of n.

With our assumptions in hand, we can now state our main theorem. Our theorem relates the uniformity of the spectrum of X to the quasiconvexity of $\mathcal{L}$. As we have shown in Proposition 2, the scaling of the singular values does not matter for the quasiconvexity of $\mathcal{L}$. We therefore take the spectrum to be nearly uniform around $\mathbf{1} \in \mathbb{R}^D$.

Theorem 1. *Consider a series of regression problems with N growing to infinity, where the Nth problem uses data $(X^{(N)}, Y^{(N)})$. Assume this sequence satisfies Assumptions 1 to 4. Let the covariate matrix of the Nth regression problem have SVD $X^{(N)} = U^{(N)} \operatorname{diag}(S^{(N)}) V^{(N)}$. There is a $N_0 > 0$ and neighborhood Δ of $\mathbf{1} \in \mathbb{R}^D$ such that if $N \geq N_0$ and the spectrum $S^{(N)} \in \Delta$, then $\mathcal{L}$ is quasiconvex.*

Proof sketch: For one-dimensional functions $\mathcal{L}$, a sufficient condition for quasiconvexity is that for all λ such that $\mathcal{L}'(\lambda) = 0$, we have $\mathcal{L}''(\lambda) > 0$ [Boyd and Vandenberghe, 2009, Chapter 3.4]. We first show $\mathcal{L}'$ can be zero only for a bounded set of λ. We then show that for any λ within this set with $\mathcal{L}'(\lambda) = 0$, we have $\mathcal{L}''(\lambda) > 0$. See Appendix E for a full proof. □

In Section 4, we showed it can be difficult to guess when $\mathcal{L}$ is quasiconvex. But Theorem 1 yields one condition that guarantees $\mathcal{L}$ is quasiconvex: when X has a nearly uniform spectrum. A natural question then is: when is the spectrum of X nearly uniform? As it happens, a uniform spectrum occurs under standard assumptions, for example, when the x_{nd} are i.i.d. sub-Gaussian random variables.

Definition 3 (e.g. [Vershynin, 2018]). *A random variable Q is sub-Gaussian if there exists a constant $c > 0$ such that $\mathbb{E}[\exp\left(Q^2/c^2\right)] \leq 2$.*

Corollary 1. *Take any series of regression problems satisfying Assumptions 3 and 4. Assume the series of regression problems are drawn from a well-specified linear model for some $\theta^* \in \mathbb{R}^D$: $y_n^{(N)} = \langle x_n^{(N)}, \theta^* \rangle + \varepsilon_n$, where $\varepsilon_n \overset{i.i.d.}{\sim} \mathcal{N}(0, \sigma^2)$. If σ is sufficiently small, $\hat{\theta}$ is consistent for θ^*, and the entries of the covariate matrices $x_{nd}^{(N)}$ are i.i.d. sub-Gaussian random variables, then $\mathcal{L}$ is quasiconvex with probability tending to 1 as $N \to \infty$.*

Proof sketch: Assumptions 1 and 2 hold for a well-specified linear model. If the entries of X are i.i.d. sub-Gaussian random variables, standard concentration inequalities imply that its spectrum is nearly uniform with high probability; hence the result of Theorem 1 applies. See Appendix F for a full proof. □

6 Theorem 1 in practice

In Section 5, we established a number of assumptions that we then required in Theorem 1 to prove that $\mathcal{L}$ is quasiconvex. A few questions remain about our theorem in practice: (1) how large is the neighborhood Δ, (2) how necessary are our assumptions, and (3) how large do we require N to be? We explicitly answer (1) and (2) with experiments below. (3) is particularly concerning, as regularization has minimal impact when $N \gg D$. That is, there is little performance gain by using a regularizer, which removes the need for hyperparameter tuning. To show that our theorem holds when $N \sim D$, the majority of our experiments validating Theorem 1 use N that is at most an order of magnitude larger than D.

Throughout our experiments, we check for non-quasiconvexity numerically and use a shortcut formula to compute $\mathcal{L}$ that takes advantage of the fact that the right singular vectors of X are $V = I_D$; see Appendix I for details. The only software dependency for our experiments is NumPy [Harris et al., 2020], which uses the BSD 3-Clause "New" or "Revised" License.

How do we know S is in the neighborhood Δ in Theorem 1? While our theorem does not give an explicit size of the neighborhood Δ, we can show empirically that Δ is substantial, even for small to moderate N. We fix $D = 5$. To generate various spectra of X, we set $S_d = e^{\alpha d}/e^{\alpha D}$. For $\alpha \to 0$, we get $S \to \mathbf{1}$; we vary α from zero to one to generate spectra of varying distances from uniformity. For each α, we sample 100 left-singular-value matrices U from the uniform distribution over orthonormal U with column means equal to 0; see Appendix G for how to generate such matrices. We fix a unit-norm $\theta^* \in \mathbb{R}^D$ and for each U, we generate data from a well-specified linear model, $y_n = \langle x_n, \theta^* \rangle + \varepsilon_n$, where the ε_n are drawn i.i.d. from $\mathcal{N}(0, \sigma^2)$ with variance $\sigma^2 = 0.5$. In particular, for each setting of U, we generate 100 vectors Y. For each setting of U and Y, we compute $\mathcal{L}$ and check whether it is quasiconvex. In the top left panel of Fig. 3, we report the fraction of problems (out of the $100 * 100 = 10,000$ datasets for the corresponding α value) with a non-quasiconvex $\mathcal{L}$ versus the distance from uniformity, $\|S - \mathbf{1}\|_1$. We see that, even for $N = 20$, the fraction of non-quasiconvex problems quickly hits zero as $\|S - \mathbf{1}\|_1$ shrinks.

To provide a rough practical heuristic, we observe from Fig. 3 that when $N = 50$ and $\|S - \mathbf{1}\|_1 \sim 2$, non-quasiconvexity occurs less than 1% of the time. In Fig. 3, Δ appears to grow slightly with N, so Fig. 3 seems to suggest that we should expect to see little quasiconvexity if $\|S - \mathbf{1}\|_1 \leq 2$ and $N \geq 50$. In practice, how should we access the spectrum to check this condition? When N and D are small enough we can directly compute S via the singular value decomposition; however, in practice, N or D may be large. If N is large and D is small, we can access the spectrum as the square root
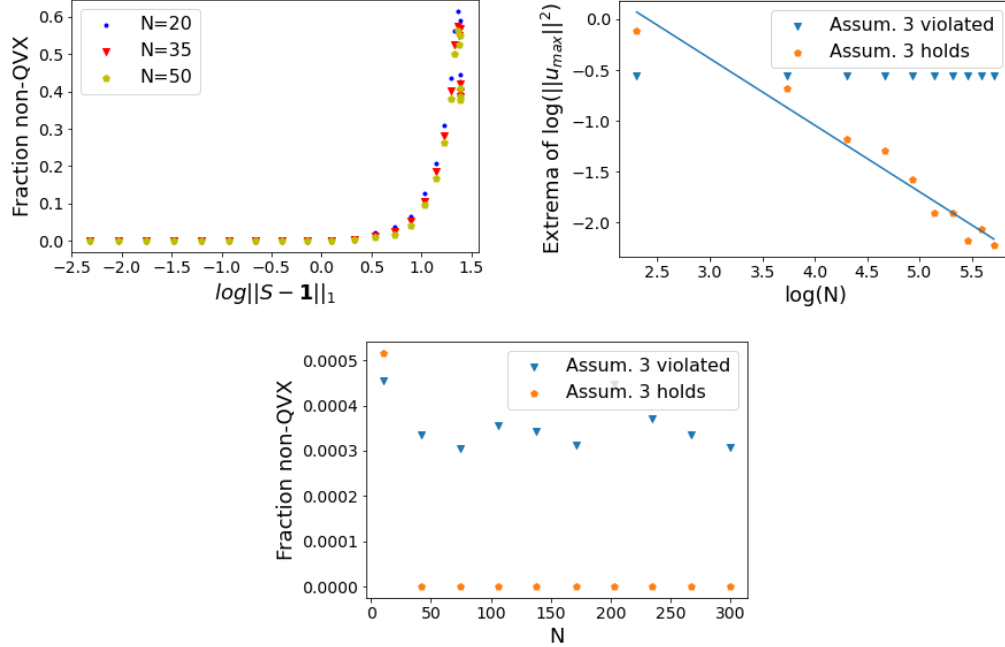
Figure 3: (*Upper left*): We generate many datasets and plot the fraction that are non-quasiconvex ("non-QVX"), varying N and the distance of the spectrum from uniformity ($\|S - \mathbf{1}\|_1$). (*Upper right*): We generate two sets (orange, blue) of left-singular vector matrices U. In the blue case, we check that the maximum of $\log \|u_{\max}\|^2$ across all U for a particular N decreases roughly linearly on a log-log plot (i.e. the blue set satisfies Assumption 3). In the orange case, we check that the minimum of $\log \|u_{\max}\|^2$ across all U for a particular N is roughly constant (i.e. the orange set does not satisfy Assumption 3). (*Lower*): For all the U matrices from the upper right plot, we generate many datasets and plot the fraction that are not quasiconvex.

of the eigenvalues of $X^T X$. If N is *very* large, formation of $X^T X$ can be expensive; in this case, we suggest the use of randomized sketching to obtain a randomized approximation to the spectrum of X [Woodruff et al., 2014]. Finally, when both N and D are large, we can use spectral density estimation, which gives an estimate of the density of a matrix's eigenvalues [Lin et al., 2016], and has been shown to successfully scale to large problems [Ghorbani et al., 2019, Yao et al., 2020].

Importance of Assumption 3. We now establish the necessity of Assumption 3 on the decay of $\|u_{\max}\|^2$ with N. To do so, we generate two sets of matrices U as N grows. We generate the first set to satisfy Assumption 3, and we generate the second to violate Assumption 3. In both cases, we will take $D = 5$ and ten settings of N between $N = 10$ and $N = 300$.

To generate the assumption-satisfying matrices U, we proceed as follows. For each N, we draw 500 matrices U from the uniform distribution over orthonormal U matrices with column means equal to 0. For each N, we plot the *maximum* value of $\|u_{\max}\|^2$ across these 500 U matrices in Fig. 3 (top-right) as a blue dot. We fit a line to these values on a log-log plot, and find the slope is -0.74. This confirms that these matrices satisfy Assumption 3.

To generate assumption-violating matrices U, we proceed as follows. Recall that the smallest N is 10 and $D = 5$. 100 times, we randomly draw a $U_{\text{small}} \in \mathbb{R}^{8 \times 5}$. We then construct each U by appending $N - 8 \times D$ zeros to U_{small}. For each N, we plot the *minimum* value of $\|u_{\max}\|^2$ across these 100 U matrices in Fig. 3 (top-right) as an orange dot. Since the minimum of $\|u_{\max}\|^2$ is constant with N, Assumption 3 is violated.

Now we check quasiconvexity. To that end, we randomly select a fixed unit-norm vector $\theta^* \in \mathbb{R}^D$. For each N, we generate 100 noise vectors $E \in \mathbb{R}^N$, where the entries E_n are drawn i.i.d. from $\mathcal{N}(0, 0.5)$. For each U and E, we construct $Y = US\theta^* + E$, where $S = \mathbf{1} \in \mathbb{R}^D$. We then compute the fraction of these $(100 * 100 = 10{,}000)$ losses $\mathcal{L}$ that are non-quasiconvex. In the lower panel
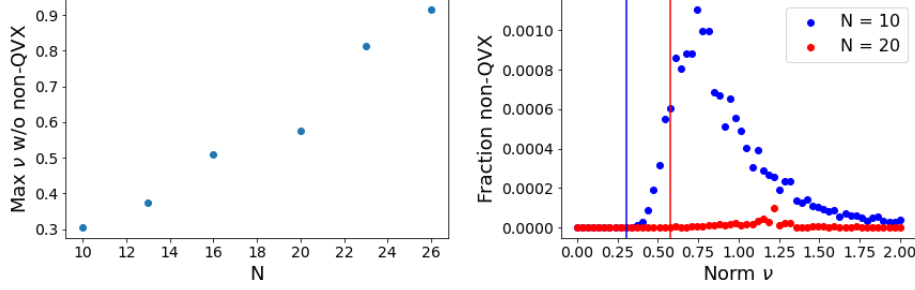
Figure 4: Checking Assumption 1. (*Left*): For each N and each $\nu = \|\hat{E}\|$, we generate many datasets and check if there is any non-quasiconvex ("non-QVX") $\mathcal{L}$. We plot the largest ν for which we find only quasiconvex $\mathcal{L}$. The growth is roughly linear, which suggests Assumption 1 cannot be loosened. (*Right*): For each N and each $\nu = \|\hat{E}\|$, we generate many data sets and plot the fraction of $\mathcal{L}$ that are non-quasiconvex. Vertical lines show ν_{max} for each N.

of Fig. 3, we plot this fraction against N for both for the assumption-satisfying case (blue) and the assumption-violating case (orange) in Assumption 3. When the assumption is satisfied (blue), we see that the conclusion of Theorem 1 holds: beyond a certain N, there are no settings of U or Y that generate a non-quasiconvex $\mathcal{L}$. We see that in practice, the boundary N is small or moderate (below 50). When the assumption is violated (orange dots), we see that the conclusion of Theorem 1 fails to hold: as N grows, there are still settings of U and Y for which quasiconvexity fails to hold. Finally, we call attention to the vertical axis. Even in the assumption-violating case, the fraction of non-quasiconvex losses is small. It follows that, even for our degenerate U's, nearly every combination of noise and U leads to a quasiconvex $\mathcal{L}$. An interesting challenge for future work is to provide a precise characterization of this effect.

Do the $\hat{\varepsilon}_n$ need to be small (Assumption 1)? Finally, we demonstrate the necessity of Assumption 1, which can be restated as requiring that $\|\hat{E}\|^2$ grows at most linearly in N. But we also find a suggestion that there may be even more permissive assumptions of interest. To this end, we vary N from 10 to 30. For each N, we generate 4,000 settings of U, each uniform over orthonormal U with column means equal to 0. For each U, we generate 250 unit vectors R such that $U^T R = 0$ (each generated uniformly over such R; see Appendix G). Separately, we consider 60 different norms ν for the vector $\hat{E}$ equally spaced between $\nu = 0$ and $\nu = 2$; these are the same across N. We generate a single unit-norm $\theta^* \in \mathbb{R}^D$.

For each setting of U, R, and ν, we consider the regression problem with covariate matrix $U\mathbf{1}$ and responses $Y = U\mathbf{1}\theta^* + \hat{E}$, where $\hat{E} := \nu R$. We record whether $\mathcal{L}$ is quasiconvex or not for this problem. For a particular N and particular error-norm ν, we check whether *any* of the $\mathcal{L}$ (across $4,000 * 250 = 1,000,000$ problems) were non-quasiconvex. Finally, for each N, we find the maximum error-norm $\nu_{\max,N}$ such that for all $\nu < \nu_{\max,N}$ every regression problem is quasiconvex. We plot a dot at $(N, \nu_{\max,N})$ in the left panel of Fig. 4. We see that in fact the boundary of allowable $\hat{E}$ norms does grow about linearly in N.

Our next plot lends additional insight into how the boundary $\nu_{\max,N}$ varies with N and is also suggestive of other potential variations on Assumption 1 that might be of interest. In particular, in the right panel of Fig. 4, we consider two particular values of N: $N = 10$ (blue) and $N = 20$ (red). For each setting of ν on the horizontal axis, we compute the fraction of non-quasiconvex losses $\mathcal{L}$ over all settings of U and R ($4,000 * 250 = 1,000,000$ problems for each ν). We see that, as expected from the left panel of Fig. 4, the boundary $\nu_{\max,N}$ is higher for $N = 20$ than for $N = 10$. Surprisingly, we also see that at high values of ν, the fraction of non-quasiconvex cases decreases again. We conjecture that in general (i.e. beyond these two particular N), large amounts of noise leads to little or no non-quasiconvexity. Finally, we note that, as in the bottom panel of Fig. 3, the fraction of non-quasiconvex cases across all ν is low. Again, this small fraction suggests a direction for future work.

7   Discussion

We have shown that the LOOCV loss $\mathcal{L}$ for ridge regression can be non-quasiconvex in real-data problems. Local optima need not be global optima. These multiple local optima may pose a practical problem for common hyperparameter tuning methods like gradient-based optimizers, which may get stuck in a local optimum, and grid search, for which upper and lower bounds need to be set.

We proved that the quasiconvexity of $\mathcal{L}$ is determined by only a few aspects of a linear regression problem. But we also showed that the quasiconvexity of $\mathcal{L}$ is still a complicated function of the remaining quantities, and as of this writing the nature of this function is far from fully understood. Nonetheless, we have provided theory that guarantees at least some useful cases when $\mathcal{L}$ is quasiconvex: when the spectrum of the covariate matrix is sufficiently flat, the least-squares fit $\hat{\theta}$ fits the data reasonably well, and the left singular vectors of the covariate matrix are regular. In our experiments, we have confirmed that these assumptions are necessary to some extent: when they are not satisfied, $\mathcal{L}$ can be non-quasiconvex. Still, our empirical results make it clear there is more to be explored. We describe some of the directions we believe are most interesting for future work below.

Sharper characterization of when $\mathcal{L}$ is quasiconvex. Fig. 2 shows that non-quasiconvexity disappears as the spectrum of X becomes uniform; however, it is clear that there is very regular behavior to the pattern of quasiconvexity even when the singular values of X are non-uniform. We are not able to characterize these patterns at this time but believe these patterns pose a fascinating challenge for future work. Relatedly, our experiments (Section 6) show that when our assumptions are violated, quasiconvexity of $\mathcal{L}$ is not guaranteed. However, we have observed that even when $\mathcal{L}$ is not guaranteed to be quasiconvex, many settings of U and Y still give quasiconvexity. In many of our experiments, the fraction of non-quasiconvex losses $\mathcal{L}$ was extremely small.

How many local optima and how bad are they? Without the guarantee of a single, global optimum, it is not clear that we can ever know that we have globally (near-)optimized $\mathcal{L}$. However, notice that our examples in Fig. 1 all have at most two local optima. In simulated experiments, we also typically encountered two local optima in non-quasiconvex losses, although we have not studied this behavior systematically. If $\mathcal{L}$ were guaranteed to have only two or some small number of optima, optimization might again be straightforward, even in the case of non-quasiconvexity; an algorithm could search until it finds the requisite number of optima and then report the one with the smallest value of $\mathcal{L}$. Alternatively, one might hope that all local optima have CV loss (and ideally out-of-sample error) close in value to that of the global optimum. Indeed, Kawaguchi [2016] argue that this property holds for certain losses in deep learning. Presumably it is not universally the case that local optima exhibit similar loss since the right panel of Fig. 1 seems to give a counterexample. But it might be widely true, or true under mild conditions. Meanwhile, in the absence of such guarantees, optimization of $\mathcal{L}$ should proceed with caution.

Beyond ridge regression. We have shown – in our opinion – surprising non-quasiconvexity for the LOOCV loss for ridge regression. Do similar results hold for simple models outside ridge regression? The regularization parameter in other ℓ_2 or ℓ_1-regularized generalized linear models is often tuned by minimizing a cross-validation loss. In preliminary experiments, we have found non-quasiconvexity in ℓ_2-regularized logistic regression. To what extent do empirical results like those in Fig. 2 or theoretical results like those in Theorem 1 hold for other models and regularizers?

Acknowledgements

References

D. M. Allen. The relationship between variable selection and data agumentation and a method for prediction. *Technometrics*, 16(1):125–127, Feb 1974.

J. Bergstra and Y. Bengio. Random search for hyper-parameter optimization. *Journal of Machine Learning Research*, 13(2), 2012.

C. M. Bishop. *Pattern Recognition and Machine Learning*. Springer, 2006.

S. Boyd and L. Vandenberghe. *Convex Optimization*. Cambridge University Press, 2009.

E. J. Candés and B. Recht. Exact matrix completion via convex optimization. *Foundations of Computational Mathematics*, 9, 2009.

D. Chetverikov, Z. Liao, and V. Chernozhukov. On cross-validated Lasso in high dimensions. *arXiv Preprint*, February 2020.

P. Cortez, A. Cerdeira, F. Almeida, T. Matos, and J. Reis. Modeling wine preferences by data mining from physicochemical properties. https://archive.ics.uci.edu/ml/datasets/wine+quality, 2009a. Accessed November 12, 2020.

P. Cortez, A. Cerdeira, F. Almeida, T. Matos, and J. Reis. Modeling wine preferences by data mining from physicochemical properties. *Decision Support Systems*, 47(4):547–553, 2009b.

C. B. Do, C. Foo, and A. Y. Ng. Efficient multiple hyperparameter learning for log-linear models. In *Neural Information Processing Systems (NIPS)*, 2007.

Behrooz Ghorbani, Shankar Krishnan, and Ying Xiao. An investigation into neural net optimization via Hessian eigenvalue density. In *International Conference on Machine Learning*, pages 2232–2241. PMLR, 2019.

C. R. Harris, K. Jarrod Millman, S. J. van der Walt, R. Gommers, P. Virtanen, David C. Cournapeau, E. Wieser, J. Taylor, S. Berg, N. J. Smith, R. Kern, M. Picus, S. Hoyer, M. H. van Kerkwijk, M. Brett, A. Haldane, J. Fernández del Río, M. Wiebe, P. Peterson, P. Gérard-Marchant, K. Sheppard, T. Reddy, W. Weckesser, H. Abbasi, C. Gohlke, and T. E. Oliphant. Array programming with NumPy. *Nature*, 585(7825):357–362, September 2020.

T. Hastie, R. Tibshirani, and M. Wainwright. *Statistical learning with sparsity: the Lasso and generalizations*. Chapman and Hall / CRC, 2015.

T. Hastie, R. Tibshirani, and J. Friedman. *The Elements of Statistical Learning*. Springer, Jan 2017.

T. Hastie, A. Montanari, S. Rosset, and R. J. Tibshirani. Surprises in high-dimensional ridgeless least squares interpolation. *arXiv preprint*, Dec 2020.

D. Homrighausen and D. J. McDonald. The lasso, persistence, and cross-validation. In *International Conference in Machine Learning (ICML)*, 2013.

D. Homrighausen and D. J. McDonald. Leave-one-out cross-validation is risk consistent for Lasso. *Machine Learning*, 97(1-2):65–78, October 2014.

C. Hsu, C. Chang, and C. Lin. A practical guide to support vector classification, 2003.

K. Kawaguchi. Deep learning without poor local minima. In *Neural Information Processing Systems (NIPS)*, 2016.

Lin Lin, Yousef Saad, and Chao Yang. Approximating spectral densities of large matrices. *SIAM review*, 58(1):34–65, 2016.

J. Lorraine, P. Vicol, and D. Duvenaud. Optimizing millions of hyperparameters by implicit differentiation. In *International Conference on Artificial Intelligence and Statistics (AISTATS)*, 2020.

D. Maclaurin, D. Duvenaud, and R. P. Adams. Gradient-based hyperparameter optimization through reversible learning. In *International Conference on Machine Learning (ICML)*, 2015.

K. Musgrave, S. Belongie, and S. N. Lim. A machine learning reality check. In *European Conference on Computer Vision (ECCV)*, 2020.

P. Patil, Y. Wei, A. Rinaldo, and R. J. Tibshirani. Uniform consistency of cross-validation estimators for high-dimensional ridge regression. In *International Conference on Artificial Intelligence and Statistics (AISTATS)*, 2021.

F. Pedregosa. Hyperparameter optimization with approximate gradient. In *International Conference in Machine Learning (ICML)*, 2016.

F. Pedregosa, G. Varoquaux, A. Gramfort, V. Michel, B. Thirion, O. Grisel, M. Blondel, P. Prettenhofer, R. Weiss, and V. Dubourg. Scikit-learn: Machine learning in python. *The Journal of Machine Learning Research*, 12:2825–2830, 2011.

K. R. Rad and A. Maleki. A scalable estimate of the out-of-sample prediction error via approximate leave-one-out cross-validation. *Journal of the Royal Statistical Society Series B*, June 2020.

K. Rajarshi. Life expectancy (WHO). `https://www.kaggle.com/kumarajarshi/life-expectancy-who`, 2018. Accessed May 02, 2021.

M. Stone. Cross-validatory choice and assessment of statistical predictions. *Journal of the American Statistical Association*, 36(2):111–147, 1974.

R. Vershynin. *High-dimensional Probability: An Introduction with Applications in Data Science*. Cambridge University Press, August 2018.

A. Wilson, M. Kasy, and L. Mackey. Approximate cross-validation: guarantees for model assessment and selection. In *International Conference on Artificial Intelligence and Statistics (AISTATS)*, 2020.

David P Woodruff et al. Sketching as a tool for numerical linear algebra. *Foundations and Trends® in Theoretical Computer Science*, 10(1–2):1–157, 2014.

Zhewei Yao, Amir Gholami, Kurt Keutzer, and Michael W Mahoney. Pyhessian: Neural networks through the lens of the Hessian. In *2020 IEEE International Conference on Big Data*, pages 581–590. IEEE, 2020.

Checklist

1. For all authors...
   (a) Do the main claims made in the abstract and introduction accurately reflect the paper's contributions and scope? [Yes]
   (b) Did you describe the limitations of your work? [Yes] See Section 7.
   (c) Did you discuss any potential negative societal impacts of your work? [No] Our work focuses on pointing out flaws with existing methodology and understanding when these flaws do not occur. As these flaws exist independent of any kind of malicious action, it is hard for us to find any negative societal impact of our work.
   (d) Have you read the ethics review guidelines and ensured that your paper conforms to them? [Yes]

2. If you are including theoretical results...
   (a) Did you state the full set of assumptions of all theoretical results? [Yes]
   (b) Did you include complete proofs of all theoretical results? [Yes] We refer to the relevant part of the appendix after each stated result.

3. If you ran experiments...
   (a) Did you include the code, data, and instructions needed to reproduce the main experimental results (either in the supplemental material or as a URL)? [Yes]
   (b) Did you specify all the training details (e.g., data splits, hyperparameters, how they were chosen)? [Yes]
   (c) Did you report error bars (e.g., with respect to the random seed after running experiments multiple times)? [Yes] See Appendix H for our experiments replicated with error bars.
   (d) Did you include the total amount of compute and the type of resources used (e.g., type of GPUs, internal cluster, or cloud provider)? [No] As we are not proposing a new method that others might use themselves, we do not think compute time is relevant in our experiments.

4. If you are using existing assets (e.g., code, data, models) or curating/releasing new assets...

    (a) If your work uses existing assets, did you cite the creators? [Yes]

    (b) Did you mention the license of the assets? [Yes] See Section 6.

    (c) Did you include any new assets either in the supplemental material or as a URL? [N/A] We do not create new assets besides the code from question 3a.

    (d) Did you discuss whether and how consent was obtained from people whose data you're using/curating? [Yes] See Appendix A.

    (e) Did you discuss whether the data you are using/curating contains personally identifiable information or offensive content? [Yes] See Appendix A.

5. If you used crowdsourcing or conducted research with human subjects...

    (a) Did you include the full text of instructions given to participants and screenshots, if applicable? [N/A] We do not use crowdsourcing or human subjects.

    (b) Did you describe any potential participant risks, with links to Institutional Review Board (IRB) approvals, if applicable? [N/A] We do not use crowdsourcing or human subjects.

    (c) Did you include the estimated hourly wage paid to participants and the total amount spent on participant compensation? [N/A] We do not use crowdsourcing or human subjects.

A   Real dataset descriptions

Here, we give the details for the real datasets used to generate Fig. 1.

Life expectancy.   Our first real dataset contains $N = 2{,}938$ observations of life expectancy in a country, along with $D = 20$ covariates such as country of origin or alcohol use. The dataset is available from [Rajarshi, 2018]. In this case, $\mathcal{L}$ for the full dataset is quasiconvex. But now consider some standard data pre-processing. Practitioners often perform principal component regression (PCR) with the aim of reducing noise in the estimated θ. That is, they take the singular value decomposition of $X = USV$; they then produce an $N \times R$ dimensional covariate matrix X' by retaining just the upper R singular values of X: $X' = U_{.,:R}S_{:R}$. If we include this pre-processing step, the resulting LOOCV curve $\mathcal{L}$ is non-quasiconvex for many values of R; in the center panel of Fig. 1 we show one example for $R = 15$.

This dataset does contain information about people. However, it is only reported at the aggregated level by a given country per year. It is not clear to us whether or not consent was obtained by the individuals living in these countries; however, we feel the publication of such data is unlikely to negatively affect any given individual. Additionally, while we do not know if the data reveals any identifying information about an individual, we feel it is unlikely to do so, as it is published at the country level.

Wine dataset.   Our second dataset consists of recorded wine quality of $N = 1{,}599$ red wines. The goal is to predict wine quality from $D = 11$ observed covariates relating to the chemical properties of each wine [Cortez et al., 2009a,b]. We find that subsets of this dataset often exhibit non-quasiconvex $\mathcal{L}$. We search over 400 random subsets of this dataset of size $N = 50$. In Fig. 1. Twelve of these led to non-quasiconvex losses $\mathcal{L}$, and Fig. 1 shows one of these examples.

This dataset does not contain information about people, and so concerns about consent and personally identifying information do not seem relevant here.

B   Proof of Proposition 2

We now restate and then prove Proposition 2.

Proposition 2. *Assume Condition 1 holds. The quasiconvexity of $\mathcal{L}$ is independent of the following*

   1. *The matrix of right singular vectors, V*

   2. *The norm of the responses, $\|Y\|_2$*

   3. *The scaling of the singular values (i.e. changing S into S/c for $c \in \mathbb{R}_{>0}$)*

in the sense that altering any of these quantities does not change whether or not $\mathcal{L}$ is quasiconvex.

Proof.   First, it is easiest to write our function of interest in a simpler form:

$$\mathcal{L}(\lambda) = \sum_{n=1}^{N} \frac{1}{(1 - Q_n(\lambda))^2}(x_n^T \hat{\theta}_\lambda - y_n)^2, \tag{4}$$

where $Q_n(\lambda) := x_n^T \big(X^T X + \lambda I_D\big)^{-1} x_n$ and $\hat{\theta}_\lambda := \big(X^T X + \lambda I_D\big)^{-1} X^T Y$.

Let the singular value decomposition of X be $X = U \operatorname{diag}(S)V$. Then:

V does not affect does not affect the quasiconvexity of $\mathcal{L}$.   To prove this claim, note that $x_n = u_n^T \operatorname{diag}(S)V$, where u_n is the nth row of U. So:

$Q_n(\lambda) = u_n^T \operatorname{diag}(S)V^T \big(V \operatorname{diag}(S^2 + \lambda)^{-1}V^T\big)V \operatorname{diag}(S)u_n = u_n^T \operatorname{diag}(S) \operatorname{diag}(S^2 + \lambda)^{-1} \operatorname{diag}(S)u_n.$

So $Q_n(\lambda)$ is actually independent of V. Next,

$$x_n^T \hat{\theta}_\lambda = u_n^T \operatorname{diag}(S)V^T V \operatorname{diag}(S^2 + \lambda)^{-1}V^T V \operatorname{diag}(S)U^T Y$$
$$= u_n^T \operatorname{diag}(S) \operatorname{diag}(S^2 + \lambda)^{-1} \operatorname{diag}(S)U^T Y,$$

which is also independent of V.

$\|\mathbf{Y}\|_2^2$ **does not affect the quasiconvexity of** $\mathcal{L}$**.** In particular, we can treat Y as sitting on the D-dimensional unit sphere. To see this, take two different Y's related by a scaling: $y_n^{(1)} = c y_n^{(0)}$ for some scalar $c \in \mathbb{R}$. Then, using the same superscripts:

$$\hat{\theta}_\lambda^{(1)} = \left(X^T X + \lambda I_D\right)^{-1} X^T Y^{(1)} = c\hat{\theta}_\lambda^{(0)}.$$

So, we can relate the two LOOCV functions by:

$$\mathcal{L}^{(1)}(\lambda) = \sum_n \frac{1}{(1 - Q_n(\lambda))^2} \left(c x_n^T \hat{\theta}_\lambda^{(0)} - c y_n^{(0)}\right)^2 = c^2 \mathcal{L}^{(0)}(\lambda). \tag{5}$$

So scaling Y by c uniformly scales $\mathcal{L}(\lambda)$ by c^2. Mutliplying $\mathcal{L}$ by a constant does not affect is quasiconvexity.

The scaling of the singular values $s_1, \ldots, s_D$ **does not affect the quasiconvexity of** $\mathcal{L}$**.** We have already shown that V does not affect the quasiconvexity of $\mathcal{L}$, so fix $V = I_D$ to simplify the proof. Pick some scaling $c > 0$, and fix some spectrum $S^{(1)}$. Define $S^{(0)} := cS^{(1)}$. Using the same superscripts, we have:

$$Q_n^{(0)}(\lambda) = \sum_{d=1}^D u_{nd}^2 \frac{c^2 s_d^2}{c^2 s_d^2 + \lambda} = \sum_{d=1}^D u_{nd}^2 \frac{s_d^2}{s_d^2 + (\lambda/c^2)} = Q^{(1)}\left(\frac{\lambda}{c^2}\right) \tag{6}$$

Similarly, define $(x_n^T \hat{\theta})^{(0)}(\lambda)$ to be the inner product of $x_n^{(0)}$ and $\hat{\theta}^{(0)}(\lambda)$. Then:

$$(x_n^T \hat{\theta})^{(0)}(\lambda) = u_n^T \operatorname{diag}(S^{(0)})\left(\operatorname{diag}(S^{(0)})^2 + \lambda I_D\right)^{-1} \operatorname{diag}(S^{(0)}) U^T Y \tag{7}$$

$$= u_n^T \operatorname{diag}(S^{(1)})\left(\operatorname{diag}(S^{(1)})^2 + \frac{\lambda}{c^2} I_D\right)^{-1} \operatorname{diag}(S^{(1)}) U^T Y \tag{8}$$

$$= (x_n^T \hat{\theta})^{(1)}\left(\frac{\lambda}{c^2}\right). \tag{9}$$

This, along with Eq. (6) implies that $\mathcal{L}^{(0)}(\lambda) = \mathcal{L}^{(1)}(\lambda/c^2)$. That is, multiplying the singular values by c stretches out $\mathcal{L}$ by a factor of c. This does not change the quasiconvexity of $\mathcal{L}$. $\square$

C Measuring severity of non-quasiconvexity with other losses and optimization methods

Fig. 2 shows the severity of non-quasiconvexity when searching over all possible $N = 3, D = 2$ regression problems for a fixed spectrum S. Recall that we measured the *severity* of non-quasiconvexity as

$$\text{severity} := \frac{\mathcal{L}(\lambda_{\text{worst-min}}) - \mathcal{L}(\lambda^*)}{\mathcal{L}(\lambda_{\text{worst}}) - \mathcal{L}(\lambda^*)}, \tag{10}$$

where λ_{worst}, λ^*, and $\lambda_{\text{worst-min}}$ are the λ maximizing $\mathcal{L}$, the λ minimizing $\mathcal{L}$, and the λ corresponding to the local minimum with largest $\mathcal{L}$, respectively. Eq. (10) measures the relative quality of the optima found by a hypothetical optimizer that always finds the worst possible local optimum, where the quality of an optimum is measured by $\mathcal{L}$. We view even modest values of this measure of severity as fairly severe: e.g. a severity of 0.1 indicates that the excess loss incurred by finding a bad minimum is 10% of the excess loss incurred by using the worst possible λ. Here, we investigate what happens when we replace different parts of Eq. (10).

Realistic optimization methods. First, we ask what would happen when using more realistic optimization methods. In particular, we consider replacing $\lambda_{\text{worst-min}}$ by the λ of the minimum reported by either gradient descent or grid search. For gradient descent, we have to choose a λ at which to initialize. There does not seem to be any natural data-driven heuristic to initialize gradient descent with, so we always initialize at $\lambda = 0$. For grid search, we need to choose the range of our grid and how fine a grid we will use. For the leftmost point of our grid, we use $\lambda = 0$. For the rightmost point of our grid, we use $\lambda = 2$. To justify this choice of a maximum λ, recall we have set
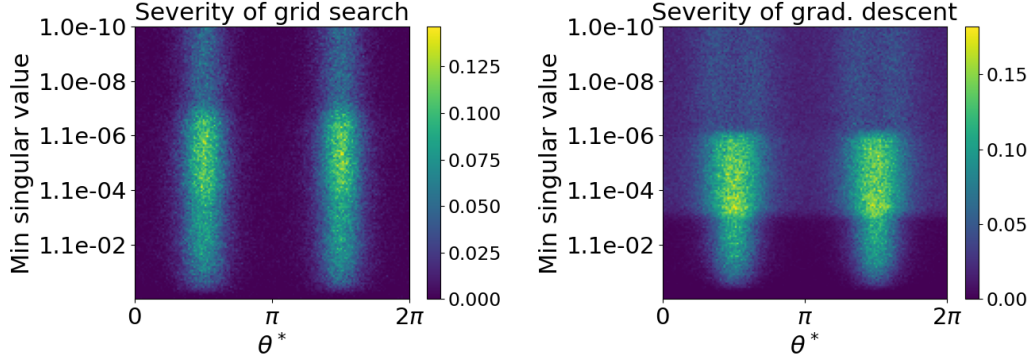
15

Figure 5: (*Left*): Severity of non-quasiconvexity where $\lambda_{\text{worst-min}}$ is the λ recovered by grid search. (*Right*): Severity of non-quasiconvexity where $\lambda_{\text{worst-min}}$ is the λ recovered by gradient descent. Note the color scales on the left and right figures differ slightly and also differ significantly from Fig. 2 in the main text.

the maximum singular value to be equal to 1. Thus $\lambda > 1$ implies that the regularizer has exceeded the scale of the covariates; it seems reasonable to not consider λ too much larger than this scale, so we select $\lambda = 2$ as our maximum. We assume that if no minimum is encountered in the range of our grid that any reasonable user would continue the grid search until finding a minimum; in such a case, we say that grid search reports the minimum with the smallest λ value. Given this range of λ's, we set our grid to be 200 λ's evenly spaced grid on the log-scale. We have never found a difference in our experiments by making this grid finer, so we expect this has no effect on the results presented here.

We could replicate the $N = 3, D = 2$ experiment of Fig. 2 using grid search and gradient descent. However, it seems that in the case of $N = 3, D = 2$, the leftmost minimum of $\mathcal{L}$ is always at some $\lambda < 1$ and is always the global optimum of $\mathcal{L}$. So, our implementations of grid search and gradient descent always find the global optimum of $\mathcal{L}$ in this case. To create examples with more interesting behavior, we instead consider the case of $N = 50, D = 2$. Here, we can still parameterize θ^* by a scalar on the unit circle, but cannot do the same for U. Instead, we vary θ^* and the singular values of X over a grid and average the severity over many random setings of U for each setting of S and θ^*. We set the singular values of X to be $S_1 = 1, S_2 = \alpha$, for some $\alpha \in (0, 1]$. We let α vary on a log-scale grid between 0 and 1 and θ^* on a grid between 0 and 2π. For each setting of α and θ^*, we construct 1000 random linear regression problems by drawing U at uniform from all zero-column-mean orthonormal matrices (Appendix G). We then set $Y = U \operatorname{diag}(S)\theta^* + E$, where $E \in \mathbb{R}^N$ has i.i.d. $\mathcal{N}(0, 0.1)$ entries. We run either grid search or gradient descent on the resulting LOOCV loss $\mathcal{L}$ and compute the severity of non-quasiconvexity via Eq. (10) with $\lambda_{\text{worst-min}}$ replaced by the λ returned by grid search or gradient descent. Finally, we average the severity over all 1000 trials. Fig. 5 visualizes the results for grid search (left) and gradient descent (right). We find that there exist settings of α and θ^* for which grid search and gradient descent typically find poor local optima. These difficulties occur for moderate values of α and when θ^* sits at an angle of around $\pi/2$ or $3\pi/2$. That is, when $\| \operatorname{diag}(S)\theta^* \| \approx \alpha$.

Other CV losses. One might ask if our finding of non-quasiconvexity is limited to leave-one-out CV. To show this is not the case, we consider the same $N = 50, D = 2$ setting as above, and again vary θ^* and α on a grid. We let $\mathcal{K}(\lambda)$ be the K-fold CV loss and compute the severity of its non-quasiconvexity as:

$$\frac{\mathcal{K}(\lambda_{\text{worst-min}}) - \mathcal{K}(\lambda^*)}{\mathcal{K}(\lambda_{\text{worst}}) - \mathcal{K}(\lambda^*)},$$

where $\lambda_{\text{worst-min}}, \lambda^*$, and λ_{worst} are the λ of the local minimum of $\mathcal{K}$ with highest loss, the global minimum of $\mathcal{K}$, and the λ maximizing $\mathcal{K}$, respectively. In the left and center of Fig. 6, we show the result for 5-fold and 10-fold CV, respectively. We find similar results as before; there are settings of θ^* and α for which the K-fold CV loss has severe non-quasiconvexity.

Test loss. Ultimately, we are hoping to find a λ such that the test loss $\mathcal{T}(\lambda)$ is small; we hope that minimizing $\mathcal{L}$ will give us such a λ. Here, we ask whether or not the presence of non-quasiconvexity
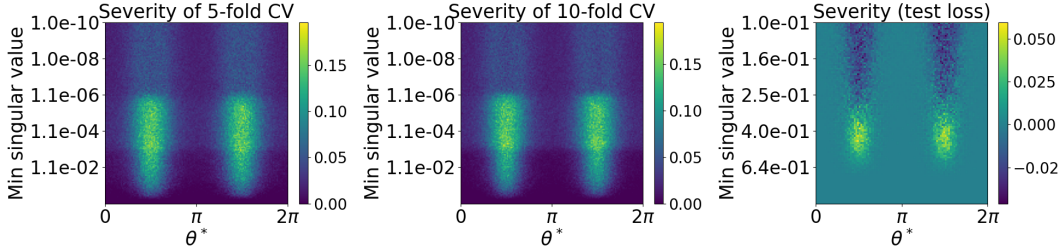
16

Figure 6: (*Left*): Severity of non-quasiconvexity in 5-fold CV. (*Centre*): Severity of non-quasiconvexity in 10-fold CV. (*Right*): Severity of non-quasiconvexity in $\mathcal{L}$, where the quality of λ_{worst}, λ^* and $\lambda_{\text{worst-min}}$ are measured using the test loss. Note that the color scale on this plot is different from that on previous plots.

in $\mathcal{L}$ can make it hard to find such a λ. Here, we define the severity of non-quasiconvexity as:

$$\frac{\mathcal{T}(\lambda_{\text{worst-min}}) - \mathcal{T}(\lambda^*)}{\mathcal{T}(\lambda_{\text{worst}}) - \mathcal{T}(\lambda^*)},$$

where $\lambda_{\text{worst-min}}$, λ^*, and λ_{worst} are the λ of the local minimum of $\mathcal{L}$ with highest loss, the global minimum of $\mathcal{L}$, and the λ maximizing $\mathcal{L}$, respectively. We use the same setup as above with $N = 50, D = 2$. The right of Fig. 6 shows the results. We see that there are settings of θ^* and α for which selecting the worst minimum of $\mathcal{L}$ typically leads to a worse test loss than does the global minimum of $\mathcal{L}$. Interestingly, there are also settings of θ^* and α for which using the worst minimum of $\mathcal{L}$ leads to a *better* test loss than the global minimum of $\mathcal{L}$ (negative values in the right of Fig. 6). We note that the absolute scale of severity under the test loss is smaller than in the other plots presented here, all of which measure the quality of a λ using CV loss. This leaves open the possibility that while different local optima may have substantively different CV losses, their performance in practice – as measured by test loss – may be fairly similar.

D   Empirical validation of Assumption 3

As noted in the main text, Assumption 3 can be interpreted as an assumption about the coherence of the U matrix, a quantity commonly found in the compressed sensing literature [Candés and Recht, 2009]. In particular, Assumption 3 requires that the coherence of U decay with N sufficiently fast. Similar conditions have been studied in the literature for other matrices. For example, Lemma 2.2 of Candés and Recht [2009] shows that if U is drawn uniformly at random from the set of all orthonormal $N \times D$ matrices, then $\max_n \|u_{\text{max}}\|^2 = O(\log(N)/N)$ with probability going to 1 as $N \to \infty$. As $\log(N)/N$ tends towards zero faster than N^{-p} for any $0 < p < 1$, Lemma 2.2 of Candés and Recht [2009] proves that Assumption 3 holds with high probability if U is drawn uniformly from the set of orthogonal matrices.

However, the U's of interest here have an additional constraint: that their columns be zero-mean. It is not clear how to adapt the proof of Candés and Recht [2009] to this situation. Instead, we offer empirical evidence that Assumption 3 holds in the case that U is drawn uniformly at random from the set of orthonormal zero-column-mean matrices. We describe how to generate such matrices in Appendix G. For fifty values of N from $N = 2,500$ to $N = 20,500$, we draw 750 orthonormal zero-mean orthonormal matrices U from the uniform distribution. We plot the average $\|u_{\text{max}}\|^2$ over these 750 replicas on a log scale versus N in Fig. 7 (orange dots). For comparison, we plot the average $\|u_{\text{max}}\|^2$ over 750 replicas when U is drawn uniformly from the set of all orthonormal matrices (no zero-mean constraint) as the blue dots. The decay of $\|u_{\text{max}}\|^2$ with and without the zero-mean constraint is essentially identical. Given this experiment, we argue that, although theoretically unjustified, Assumption 3 places only modest restrictions on the regression problems to which Theorem 1 applies.

E   Proof of Theorem 1
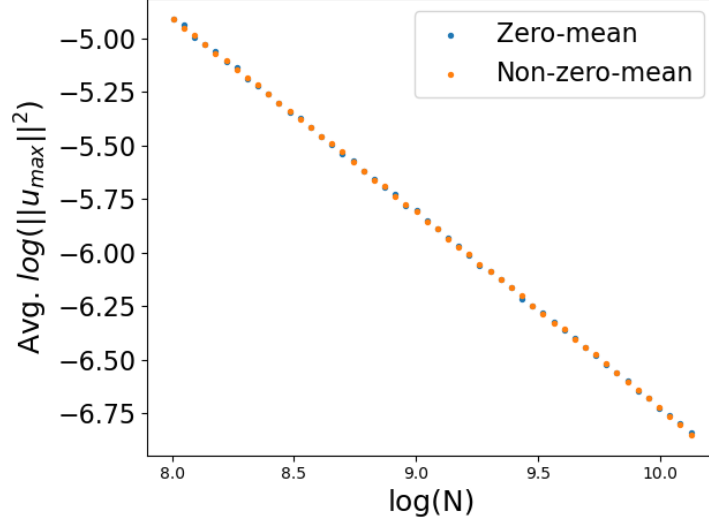
We restate and prove Theorem 1 from Section 5.

17

Figure 7: Experiment from Appendix D. Orange dots show the decay of $\|u_{\max}\|^2$ for uniformly drawn non-zero-column-mean orthonormal matrices U; we see that, as proven by Candés and Recht [2009], these matrices satisfy Assumption 3. Blue dots show the decay of $\|u_{\max}\|^2$ for uniformly drawn zero-column-mean orthonormal matrices. While such matrices are not known to satisfy Assumption 3, we see that their $\|u_{\max}\|^2$ decays at exactly the same rate as the non-zero-column-mean matrices.

Theorem 1. *Take any series of regression problems $\{X^{(N)}, Y^{(N)}\}_{N=1}^{\infty}$ satisfying Assumptions 1 to 4. Let the covariate matrix of the Nth regression problem have SVD $X^{(N)} = U^{(N)} \operatorname{diag}(S^{(N)})V^{(N)}$. There is a $N_0 > 0$ and neighborhood Δ of $\mathbf{1} \in \mathbb{R}^D$ such that if $N \geq N_0$ and the spectrum $S^{(N)} \in \Delta$, then $\mathcal{L}$ is quasiconvex.*

Proof. We first prove the theorem for an exactly uniform spectrum, $S = \mathbf{1}$. To do so, we work with a sufficient condition for a one-dimensional function $\mathcal{L}$ to be quasiconvex: for all λ such that $\mathcal{L}'(\lambda) = 0$, we have $\mathcal{L}''(\lambda) > 0$ [Boyd and Vandenberghe, 2009, Chapter 3.4]. With this characterization of quasiconvexity in mind, our proof can be broken into two steps. We sketch each step here and refer to later lemmas for their proofs.

1. **Bound the region where $\mathcal{L}'$ can be zero.** Write $\mathcal{L}'$ as:

$$\mathcal{L}'(\lambda) = \frac{1}{(\lambda+1)^4} \sum_{n=1}^{N} \frac{(\lambda+1)^3}{(\lambda+1-\|u_n\|^2)^3} \left(\xi_{n1}\lambda^2 + \xi_{n2}\lambda + \xi_{n3} \right).$$

   To find where this can be zero, we can ignore the $1/(\lambda+1)^4$. Then this is *almost* a quadratic in λ, $\sum_n \xi_{n1}\lambda^2 + \xi_{n2}\lambda + \xi_{n3}$. Find the most positive root of this quadratic, $\lambda_Q = O(1)$. Bound the deviations of $\mathcal{L}'$ away from a quadratic, and bound how far these deviations can increase the zeros $\mathcal{L}'$ beyond λ_Q. **Result:** $\mathcal{L}'(\lambda)$ can only be zero for $\lambda \in [0, \lambda_Q + o(1)]$. We prove this step in Lemma 1 below.

2. **Show $\mathcal{L}''(\lambda) > 0$ for any $\lambda \in [0, \lambda_{\mathbf{Q}} + \Theta(1)]$ for which $\mathcal{L}'(\lambda) = 0$.** Essentially the same strategy; for any $]lambda$ for which $\mathcal{L}'(\lambda) = 0$, write:

$$\mathcal{L}''(\lambda) = \frac{1}{(\lambda+1)^5} \sum_{n=1}^{N} \frac{(\lambda+1)^4}{(\lambda+1-\|u_n\|^2)^4} \left(a_n\lambda^2 + b_n\lambda + c_n \right)$$

   This is a roughly a bowl-down quadratic with only one root bigger than zero; i.e. it is positive for $\lambda \in [0, \lambda'_Q]$, where $\lambda'_Q = \lambda_Q + \Theta(1)$ is the location of the quadratic's rightmost root. Show that the deviations away from quadratic imply that $\mathcal{L}''$ is positive for $\lambda \in [0, \lambda'_Q - o(1)] = [0, \lambda_Q + \Theta(1) - o(1)]$. We prove this step in Lemma 2 below.

18

With the theorem proved for an exactly uniform spectrum, we note that $\mathcal{L}'$ and $\mathcal{L}''$ are continuous functions of the spectrum S. As $\mathcal{L}''$ is stricly bounded away from zero on a region that contains $[0, \lambda_Q + \Theta(1)]$, by continuity in the singular values, there is a neighborhood Δ of $\mathbf{1} \in \mathbb{R}^D$ such that if $S \in \Delta$, $\mathcal{L}''(\lambda) > 0$ for all λ for which $\mathcal{L}'(\lambda) = 0$. $\qquad\square$

Before getting into the proofs of our main lemmas, we can first rearrange $\mathcal{L}'$ into a convenient form. In Eq. (64) of Appendix I we gave a convenient form of $\mathcal{L}$ when the matrix of right singular vectors satisfies $V = I_D$. Setting $S = \mathbf{1} \in \mathbb{R}^D$ in Eq. (64) and then taking the derivative with respect to λ gives:

$$\mathcal{L}'(\lambda) = \sum_{n=1}^{N} \frac{2}{(1 + \lambda - \|u_n\|^2)^2} \left(\frac{1}{1+\lambda} u_n^T U^T Y - y_n \right) \tag{11}$$

$$* \left[-\frac{(1+\lambda)\|u_n\|^2}{1 + \lambda - \|u_n\|^2} \left(\frac{1}{1+\lambda} u_n^T U^T Y - y_n \right) - u_n^T U^T Y \right]$$

Let $\hat{\varepsilon}_n$ be the scalars such that $y_n = \langle x_n, \hat{\theta} \rangle + \hat{\varepsilon}_n$. Letting $\hat{E} \in \mathbb{R}^N$ be the vector with entries $\hat{\varepsilon}_n$, we have $U^T \hat{E} = 0$, and so $U^T Y = U^T U \operatorname{diag}(\mathbf{1})\hat{\theta} = \hat{\theta}$. Plugging this into Eq. (11) we get:

$$\mathcal{L}'(\lambda) = \sum_{n=1}^{N} \frac{2\left(\frac{1}{1+\lambda}\langle u_n, \hat{\theta}\rangle - \langle u_n, \hat{\theta}\rangle - \hat{\varepsilon}_n \right)}{(\lambda + 1 - \|u_n\|^2)^2} \left[-\frac{\|u_n\|^2(1+\lambda)}{\lambda + 1 - \|u_n\|^2} \left(\frac{1}{1+\lambda}\langle u_n, \hat{\theta}\rangle - \langle u_n, \hat{\theta}\rangle - \hat{\varepsilon}_n \right) - \langle u_n, \hat{\theta}\rangle - \hat{\varepsilon}_n \right]$$

$$= \sum_{n=1}^{N} \frac{2\left(-\frac{\lambda}{1+\lambda}\langle u_n, \hat{\theta}\rangle - \hat{\varepsilon}_n \right)}{(\lambda + 1 - \|u_n\|^2)^3} \left[-\|u_n\|^2(1+\lambda)\left(-\frac{\lambda}{1+\lambda}\langle u_n, \hat{\theta}\rangle - \hat{\varepsilon}_n \right) + (-\langle u_n, \hat{\theta}\rangle - \hat{\varepsilon}_n)(\lambda + 1 - \|u_n\|^2) \right]$$

Finally, rearranging to group terms multiplying λ^2 and λ, we get:

$$\mathcal{L}'(\lambda) = \frac{2}{(1+\lambda)^4} \sum_{n=1}^{N} \frac{(1+\lambda)^3}{(1 + \lambda - \|u_n\|^2)^3} \left((1 - \|u_n\|^2)\langle u_n, \hat{\theta}\rangle^2 - \|u_n\|^2\hat{\varepsilon}_n^2 + (1 - 2\|u_n\|^2)\hat{\varepsilon}_n\langle u_n, \hat{\theta}\rangle \right) \lambda^2$$

$$+ \left((1 - \|u_n\|^2)\langle u_n, \hat{\theta}\rangle^2 - 2\|u_n\|^2\hat{\varepsilon}_n^2 + (2 - 3\|u_n\|^2)\hat{\varepsilon}_n\langle u_n, \hat{\theta}\rangle \right) \lambda$$

$$+ \left(-\|u_n\|^2\hat{\varepsilon}_n^2 + (1 - \|u_n\|^2)\hat{\varepsilon}_n\langle u_n, \hat{\theta}\rangle \right) \tag{12}$$

We can write this more compactly

$$\mathcal{L}'(\lambda) = \frac{2}{(1+\lambda)^4} \sum_{n=1}^{N} \frac{(1+\lambda)^3}{(1 + \lambda - \|u_n\|^2)^3} \left(\xi_{n1}\lambda^2 + \xi_{n2}\lambda + \xi_{n3} \right), \tag{13}$$

where the ξ_i are defined by matching up coefficients between Eq. (12) and Eq. (13). Now we can prove the two main Lemmas needed to prove Theorem 1.

Lemma 1. *Take Assumptions 1 to 4. For a flat spectrum $S = \mathbf{1} \in \mathbb{R}^D$, there is some λ_Q that is $O(1)$ such that $\mathcal{L}'(\lambda) = 0$ implies that $\lambda \in [0, \lambda_Q + o(1)]$.*

Proof. First, we can discard the $1/(1+\lambda)^4$ in front of Eq. (13) for the purposes of deciding where $\mathcal{L}' = 0$; let $g(\lambda) = \mathcal{L}'(\lambda)(1+\lambda)^4$:

$$g(\lambda) = \sum_{n=1}^{N} \frac{(1+\lambda)^3}{(1 + \lambda - \|u_n\|^2)^3} \left(\xi_{n1}\lambda^2 + \xi_{n2}\lambda + \xi_{n3} \right), \tag{14}$$

Notice that g is nearly a quadratic; in particular, if $\|u_n\|^2 = 0$, then g is a quadratic. The idea is to let λ_Q be the rightmost root of this quadratic; we then show that the perturbations away from this quadratic are small enough to imply that all zeros of g lie in $[0, \lambda_Q + o(1)]$.

Write $\xi_{\cdot i} := \sum_n \xi_{ni}$. Then, via the quadratic formula, the roots of $g_Q(\lambda) := \xi_{\cdot 1}\lambda^2 + \xi_{\cdot 2}\lambda + \xi_{\cdot 3}$ are

$$\lambda = \frac{-\xi_{\cdot 2} \pm \left[\xi_{\cdot 2}^2 - 4\xi_{\cdot 1}\xi_{\cdot 3} \right]^{1/2}}{2\xi_{\cdot 1}}. \tag{15}$$

We can apply the following facts from Lemma 4: $\xi_{\cdot 1}$ and $\xi_{\cdot 2}$ are $\Theta(1)$ and $\xi_{\cdot 3}$ is negative or $o(1)$. We can conclude that the positive root of Eq. (15) is larger than the negative root and is $O(1)$; call the positive root λ_Q. Now we need to bound the devitions of g away from the quadratic g_Q. Let $\delta(\lambda) := g(\lambda) - g_Q(\lambda)$ be these deviations:

$$\delta(\lambda) := \sum_{n=1}^{N} \left(\left(\frac{\lambda+1}{\lambda+1-\|u_n\|^2} \right)^3 - 1 \right) (\xi_{n1}\lambda^2 + \xi_{n2}\lambda + \xi_{n3}). \tag{16}$$

Notice that our quadratic g_Q is convex, as $\xi_{\cdot 1} > 0$ by Lemma 4. Thus the way to move the roots of g further right than λ_Q is to have $\delta(\lambda)$ be negative. We can lower bound $\delta(\lambda) \geq \delta(0)$ by noting that $\xi_{\cdot 1}, \xi_{\cdot 2} > 0$. Thus:

$$\delta(\lambda) \geq \delta(0) = \sum_{n=1}^{N} \left(\frac{1}{(1-\|u_n\|^2)^3} - 1 \right) \left(-\|u_n\|^2 \hat{\varepsilon}_n^2 + (1-\|u_n\|^2)\hat{\varepsilon}_n \langle u_n, \hat{\theta} \rangle \right).$$

By Lemma 5, we have that $\delta(0) = o(1)$.

As we know $g(\lambda) = g_Q(\lambda) + \delta(\lambda) \geq g_Q(\lambda) + \delta(0)$, the final step of our proof is to find the right-most λ for which $g_Q(\lambda) = -\delta(0)$, as beyond such a λ, $g > 0$. In fact, an upper bound on this λ will suffice. Using convexity with the fact that $g_Q(\lambda_Q) = 0$, we have that beyond $\lambda = \lambda_Q + \delta(0)/g_Q'(\lambda_Q)$, $g_Q(\lambda) \geq \delta(0)$, and thus $g(\lambda) \geq 0$. If we knew that $g_Q'(\lambda_Q) = 2\lambda_Q \xi_{\cdot 1} + \xi_{\cdot 2}$ were $\Theta(1)$, we would be done, as:

$$\lambda_Q = \frac{\delta(0)}{g_Q'(\lambda_Q)} = \lambda_Q + \frac{\delta(0)}{2\lambda_Q \xi_{\cdot 1} + \xi_{\cdot 2}} = \lambda_Q + \frac{o(1)}{\Theta(1)} = \lambda_Q + o(1), \tag{17}$$

To see that $2\lambda_Q \xi_{\cdot 1} + \xi_{\cdot 2}$ is $\Theta(1)$, recall that we have λ_Q is $O(1)$ and positive. And by Lemma 4, $\xi_{\cdot 1}$ and $\xi_{\cdot 2}$ are positive and $\Theta(1)$. We conclude that $2\lambda_Q \xi_{\cdot 1} + \xi_{\cdot 2} = \Theta(1)$. $\qquad \square$

Lemma 2. *Take Assumptions 1 to 4. Let λ_Q be as defined in Lemma 1, and assume the covariate matrix X has a flat spectrum $S = \mathbf{1} \in \mathbb{R}^D$. Then for any $\lambda \in [0, \lambda_Q + \Theta(1)]$ such that $\mathcal{L}'(\lambda) = 0$, it holds that $\mathcal{L}''(\lambda) > 0$.*

Proof. The strategy is similar to the proof of Lemma 1: we show that $\mathcal{L}''$ is nearly a quadratic, find the root of this quadratic, and then show that the location of this root can only change by $o(1)$ due to the deviations away from quadratic.

First, we need to compute $\mathcal{L}''$. Differentiating $\mathcal{L}'$ as given by Eq. (13) gives:

$$\mathcal{L}''(\lambda) = \frac{2}{1+\lambda} \sum_{n=1}^{N} \left(-\frac{\xi_{n1}\lambda^2 + \xi_{n2}\lambda + \xi_{n3}}{(1+\lambda)(1+\lambda-\|u_n\|^2)^3} - \frac{3(\xi_{n1}\lambda^2 + \xi_{n2}\lambda + \xi_{n3})}{(\lambda+1-\|u_n\|^2)^4} \right. \tag{18}$$

$$\left. + \frac{2\xi_{n1}\lambda + \xi_{n2}}{(\lambda+1-\|u_n\|^2)^3} \right) \tag{19}$$

Now, the first term in this sum is exactly $\mathcal{L}'(\lambda)$. By the conditions of the lemma, we have that this term sums to zero. Using this fact and some algebra, we can see that $\mathcal{L}''$ is also almost a quadratic:

$$\mathcal{L}''(\lambda) = \frac{2}{(1+\lambda)^5} \sum_{n=1}^{N} \frac{(1+\lambda)^4}{(1+\lambda-\|u_n\|^2)^4} \left(-\xi_{n1}\lambda^2 \right. \tag{20}$$

$$+ \left(2(1-\|u_n\|^2)\xi_{n1} - 2\xi_{n2} \right)\lambda \tag{21}$$

$$\left. + \left((1-\|u_n\|^2)\xi_{n2} - 3\xi_{n3} \right) \right), \tag{22}$$

where the ξ_{ni}'s are as defined in the proof of Lemma 1. As we are interested in the region where $\mathcal{L}'' > 0$, we can neglect the $1/(1+\lambda)^5$ factor in front; define $h(\lambda) := (1+\lambda)^5 \mathcal{L}''(\lambda)$. Now, define

the following

$$a_n := -\xi_{n1} \tag{23}$$
$$= 2\|u_n\|^2 \hat{\varepsilon}_n^2 - (1 - \|u_n\|^2)\langle u_n, \hat{\theta}\rangle^2$$

$$b_n := 2(1 - \|u_n\|^2)\xi_{n1} - 2\xi_{n2} \tag{24}$$
$$= \big(2(1 - \|u_n\|^2)^2 - (1 - \|u_n\|^2)\big)\langle u_n, \hat{\theta}\rangle^2 + \big(-2(1 - \|u_n\|^2)\|u_n\|^2 + 4\|u_n\|^2\big)\hat{\varepsilon}_n^2$$
$$+ \big(2(1 - \|u_n\|^2)(1 - 2\|u_n\|^2) - 2(2 - 3\|u_n\|^2)\big)\hat{\varepsilon}_n\langle u_n, \hat{\theta}\rangle$$

$$c_n := (1 - \|u_n\|^2)\xi_{n2} - 3\xi_{n3} \tag{25}$$
$$= (1 - \|u_n\|^2)^2\langle u_n, \hat{\theta}\rangle^2 + \big(-2(1 - \|u_n\|^2)\|u_n\|^2 + 3\|u_n\|^2\big)\hat{\varepsilon}_n^2$$
$$+ \big((1 - \|u_n\|^2)(2 - 3\|u_n\|^2) - 3(1 - \|u_n\|^2)\big)\hat{\varepsilon}_n\langle u_n, \hat{\theta}\rangle$$

$$h_Q(\lambda) := \sum_{n=1}^{N} a_n\lambda^2 + b_n\lambda + c_n \tag{26}$$

$$\delta^{(2)}(\lambda) := \sum_{n=1}^{N} \left(\left(\frac{1 + \lambda}{1 + \lambda - \|u_n\|^2}\right)^4 - 1\right)\left(a_n\lambda^2 + b_n\lambda + c_n\right). \tag{27}$$

Note that $h = h_Q + \delta^{(2)}$. Let $a_. = \sum_n a_n$, and likewise for $b_., c_.$. Application of Proposition 3 and Assumptions 1 and 3 gives:

$$c_. = \xi_{\cdot 2} - 3\xi_{\cdot 3} + o(1). \tag{28}$$

In particular, noting that $\xi_{\cdot 3} < 0$ or is $o(1)$ and $\xi_{\cdot 2}$ is $\Theta(1)$ and positive, (Lemma 4), we have $c_. > 0$ with $|c_.| > |\xi_{\cdot 3}|$ for large enough N. Now, in general h_Q will have two roots:

$$\lambda = \frac{-b_. \pm \left[b_.^2 - 4a_.c_.\right]^{1/2}}{2a_.} = \frac{b_. \mp \left[b_.^2 + 4\xi_{\cdot 1}c_.\right]^{1/2}}{2\xi_{\cdot 1}}.$$

Now, as $[b_.^2 + 4\xi_{\cdot 1}c_.]^{1/2} > b_.$, only one of these roots is positive; call this root λ_Q'. We now want to show that $\lambda_Q' - \lambda_Q = \Theta(1)$ and is positive. We have that:

$$\lambda_Q' - \lambda_Q = \frac{b_. + \xi_{\cdot 2} + [b_.^2 + 4\xi_{\cdot 1}((1 - \|u_n\|^2)\xi_{\cdot 1} - 3\xi_{\cdot 3})]^{1/2} - [\xi_{\cdot 2}^2 - 4\xi_{\cdot 1}\xi_{\cdot 3}]^{1/2}}{\xi_{\cdot 1}} \tag{29}$$

We know the denominator is positive and $\Theta(1)$ by Lemma 4 so we just need to show the numerator is $\Theta(1)$ and positive. Combining Assumption 3 with the fact that $b_.$ is positive or $o(1)$ (by Lemma 4), we have that the numerator satisfies:

$$\geq \xi_{\cdot 2} + [4\xi_{\cdot 1}^2 - 4\xi_{\cdot 1}^2 O(N^{-p}) - 12\xi_{\cdot 3}\xi_{\cdot 1}]^{1/2} - [\xi_{\cdot 2}^2 - 4\xi_{\cdot 1}\xi_{\cdot 3}]^{1/2}.$$

Now, as $\xi_{\cdot 1} = \Theta(1)$:

$$\geq \xi_{\cdot 2} + [\Theta(1) - 12\xi_{\cdot 3}\xi_{\cdot 1}]^{1/2} - \xi_{\cdot 2} - [|4\xi_{\cdot 1}\xi_{\cdot 3}|]^{1/2}.$$

By Lemma 4, $\xi_{\cdot 3}$ is either negative or $o(1)$. So the numerator satisfies:

$$\geq [\Theta(1) - 12\xi_{\cdot 3}\xi_{\cdot 1}]^{1/2} - [|4\xi_{\cdot 1}\xi_{\cdot 3}|]^{1/2},$$

which is $\Theta(1)$ and positive. Thus $\lambda_Q' - \lambda_Q$ is $\Theta(1)$ and is positive.

Finally, we need to lower bound $\delta^{(2)}(\lambda)$ on $[0, \lambda_Q + \Theta(1)]$. As $\lambda_Q = \Theta(1)$, Lemma 6 shows that $\delta^{(2)}(\lambda) = o(1)$ for all $\lambda \in [0, \lambda_Q + \Theta(1)]$. Thus for all $\lambda \in [0, \lambda_Q + O(1) - o(1)]$ for which $\mathcal{L}'(\lambda) = 0$, we have $h(\lambda) > 0$, and so $\mathcal{L}''(\lambda) > 0$. $\square$

E.1 Technical Lemmas

Lemma 3. *Take real numbers $s_1, \ldots, s_N$ and $r_1, \ldots, r_N$, where $r_n \in [\ell, u]$ and $\sum_{n=1}^{N} s_n = 0$. Then:*

$$\left|\sum_{n=1}^{N} r_n s_n\right| \leq \frac{u - \ell}{2} \sum_{n=1}^{N} |s_n|.$$

Proof. Let $s_n^+ := \max(0, s_n)$ and $s_n^- := \max(0, -s_n)$. Then the condition $\sum_n s_n = 0$ implies that $\sum_n s_n^+ = \sum_n s_n^- = (1/2) \sum_n |s_n|$. So:

$$\left| \sum_{n=1}^{N} r_n s_n \right| \le u \sum_{n=1}^{N} s_n^+ - \ell \sum_{n=1}^{N} s_n^- = \frac{u - \ell}{2} \sum_{n=1}^{N} |s_n|.$$

$\square$

Now we state a useful consequence of our above assumptions:

Proposition 3. *Take Assumptions 1 to 3. We have:*

$$\sum_{n=1}^{N} (1 - \|u_n\|^2) \hat{\varepsilon}_n \langle u_n, \hat{\theta} \rangle = o(1)$$

Proof. Notice that $\sum_n \hat{\varepsilon}_n \langle u_n, \hat{\theta} \rangle = \hat{E}^T U \hat{\theta} = 0$. So, we are trying to bound $\left| \sum_n \|u_n\|^2 \hat{\varepsilon}_n \langle u_n, \hat{\theta} \rangle \right|$. Assumption 3 implies that $\|u_n\|^2$ is $O(N^{-p})$. As $\|u_n\|^2$ is lower bounded by zero, we can apply Lemma 3 to get the upper bound:

$$\left| \sum_{n=1}^{N} \|u_n\|^2 \hat{\varepsilon}_n \langle u_n, \hat{\theta} \rangle \right| \le O(N^{-p}) \sum_{n=1}^{N} |\hat{\varepsilon}_n \langle u_n, \hat{\theta} \rangle|. \tag{30}$$

By Cauchy-Schwarz, we can upper bound the sum as:

$$\sum_n |\hat{\varepsilon}_n \langle u_n, \hat{\theta} \rangle| \le \left(\sum_{n=1}^{N} \hat{\varepsilon}_n^2 \right)^{1/2} \left(\sum_{n=1}^{N} \langle u_n, \hat{\theta} \rangle^2 \right)^{1/2} \tag{31}$$

By Assumption 1 and the fact that $\sum_n \langle u_n, \hat{\theta} \rangle^2 = \|\hat{\theta}\|^2$, we have overall:

$$\left| \sum_{n=1}^{N} \|u_n\|^2 \hat{\varepsilon}_n \langle u_n, \hat{\theta} \rangle \right| \le O(N^{-p}) O(\sqrt{N}) \left\| \hat{\theta} \right\|^2 = o(1), \tag{32}$$

where the final equality holds because by assumption, $p > 1/2$ and $\|\hat{\theta}\| = O(1)$ $\square$

Our next lemma concerns the quadratic coefficients that show up in $\mathcal{L}'$ and $\mathcal{L}''$.

Lemma 4. *Recall the definitions of the coefficients of the quadratic parts of $\mathcal{L}'$ and $\mathcal{L}''$ from our proofs above:*

$$\xi_{n1} := \left(1 - \|u_n\|^2\right) \langle u_n, \hat{\theta} \rangle^2 - \|u_n\|^2 \hat{\varepsilon}_n^2 + \left(1 - 2\|u_n\|^2\right) \hat{\varepsilon}_n \langle u_n, \hat{\theta} \rangle$$

$$\xi_{n2} := \left(1 - \|u_n\|^2\right) \langle u_n, \hat{\theta} \rangle^2 - 2\|u_n\|^2 \hat{\varepsilon}_n^2 + \left(2 - 3\|u_n\|^2\right) \hat{\varepsilon}_n \langle u_n, \hat{\theta} \rangle$$

$$\xi_{n3} := -\|u_n\|^2 \hat{\varepsilon}_n^2 + \left(1 - \|u_n\|^2\right) \hat{\varepsilon}_n \langle u_n, \hat{\theta} \rangle$$

$$a_n := -\xi_{n1}$$
$$\qquad = 2\|u_n\|^2 \hat{\varepsilon}_n^2 - (1 - \|u_n\|^2) \langle u_n, \hat{\theta} \rangle^2$$

$$b_n := 2(1 - \|u_n\|^2) \xi_{n1} - 2\xi_{n2}$$
$$\qquad = \left(2(1 - \|u_n\|^2)^2 - (1 - \|u_n\|^2)\right) \langle u_n, \hat{\theta} \rangle^2 + \left(-2(1 - \|u_n\|^2)\|u_n\|^2 + 4\|u_n\|^2\right) \hat{\varepsilon}_n^2$$
$$\qquad \quad + \left(2(1 - \|u_n\|^2)(1 - 2\|u_n\|^2) - 2(2 - 3\|u_n\|^2)\right) \hat{\varepsilon}_n \langle u_n, \hat{\theta} \rangle$$

$$c_n := (1 - \|u_n\|^2) \xi_{n2} - 3\xi_{n3}$$
$$\qquad = (1 - \|u_n\|^2)^2 \langle u_n, \hat{\theta} \rangle^2 + \left(-2(1 - \|u_n\|^2)\|u_n\|^2 + 3\|u_n\|^2\right) \hat{\varepsilon}_n^2$$
$$\qquad \quad + \left((1 - \|u_n\|^2)(2 - 3\|u_n\|^2) - 3(1 - \|u_n\|^2)\right) \hat{\varepsilon}_n \langle u_n, \hat{\theta} \rangle$$

Further, recall $\xi_{\cdot 1} := \sum_{n=1}^{N} \xi_{n1}$, and likewise for $\xi_{\cdot 2}, \xi_{\cdot 3}, a_{\cdot}, b_{\cdot}$, and $c_{\cdot}$. The following statements hold:

1. $\xi_{\cdot 1}$ is positive and $\Theta(1)$.

2. $\xi_{\cdot 2}$ is positive and $\Theta(1)$.

3. Either $b_\cdot > 0$ or $b_\cdot$ is positive and $o(1)$.

4. Either $\xi_{\cdot 3} < 0$ or $\xi_{\cdot 3}$ is positive and $o(1)$.

Proof. We prove each item below.

1. $\xi_{\cdot 1}$ is positive and $\Theta(1)$. Using Proposition 3, we have

$$\xi_{\cdot 1} = \|\hat{\theta}\|^2 - \sum_{n=1}^{N} \|u_n\|^2 (\langle u_n, \hat{\theta} \rangle^2 + \hat{\varepsilon}_n^2) + o(1) \tag{33}$$

$$\geq \|\hat{\theta}\|^2 - \sum_{n=1}^{N} \|u_n\|^2 (\langle u_n, \hat{\theta} \rangle^2 + 2\hat{\varepsilon}_n^2) + o(1) \tag{34}$$

$$= \Theta(1), \tag{35}$$

where in the final equality we have used Assumption 4.

2. $\xi_{\cdot 2}$ is positive and $\Theta(1)$. The proof of this is identical to the proof that $\xi_{\cdot 1}$ is positive and $\Theta(1)$ but with different constants.

3. Either $b_\cdot > 0$ or $b_\cdot$ is positive and $o(1)$. From the definition of b_n:

$$b_\cdot = \sum_{n=1}^{N} \|u_n\|^2 \hat{\varepsilon}_n^2 + \|u_n\|^2 \hat{\varepsilon}_n \langle u_n, \hat{\theta} \rangle - (\|u_n\|^2 - (\|u_n\|^2)^2) \langle u_n, \hat{\theta} \rangle^2$$
$$+ (\|u_n\|^2)^2 \hat{\varepsilon}_n^2 - (\|u_n\|^2 - 2(\|u_n\|^2)^2) \hat{\varepsilon}_n \langle u_n, \hat{\theta} \rangle$$

By Assumption 3, any term with $(\|u_n\|^2)^2$ sums up to $o(1)$. Thus:

$$b_\cdot = o(1) + \sum_{n=1}^{N} \|u_n\|^2 \hat{\varepsilon}_n^2 - \|u_n\|^2 \langle u_n, \hat{\theta} \rangle^2 \tag{36}$$

$$= \left(\sum_{n=1}^{N} \|u_n\|^2 \hat{\varepsilon}_n^2 \right) - O(N^{-p}) \tag{37}$$

Thus we have that $b_\cdot$ is either positive or is $o(1)$.

4. Either $\xi_{\cdot 3} < 0$ or $\xi_{\cdot 3}$ is positive and $o(1)$. By Proposition 3

$$\xi_{\cdot 3} = o(1) - \sum_{n=1}^{N} \|u_n\|^2 \hat{\varepsilon}_n^2. \tag{38}$$

So $\xi_{\cdot 3}$ is either $o(1)$ and positive or is negative.

$\square$

Lemma 5. *Take Assumptions 1 to 3. We have:*

$$\sum_{n=1}^{N} \left(\frac{1}{(1 - \|u_n\|^2)^3} - 1 \right) \left(-\|u_n\|^2 \hat{\varepsilon}_n^2 + (1 - \|u_n\|^2) \hat{\varepsilon}_n \langle u_n, \hat{\theta} \rangle \right) = o(1). \tag{39}$$

Proof. We first show that

$$-\sum_{n=1}^{N} \left(\frac{1}{(1 - \|u_n\|^2)^3} - 1 \right) \|u_n\|^2 \hat{\varepsilon}_n^2 = o(1).$$

First, note that as $0 \leq \|u_n\|^2 < 1$, this quantity is strictly negative. So, it suffices to lower bound it by a quantity that is $o(1)$. We apply the lower bound

$$-\sum_{n=1}^{N} \left(\frac{1}{(1 - \|u_n\|^2)^3} - 1 \right) \|u_n\|^2 \hat{\varepsilon}_n^2 \geq - \left(\frac{1}{(1 - \|u_{\max}\|^2)^3} - 1 \right) \|u_{\max}\|^2 \sum_{n=1}^{N} \hat{\varepsilon}_n^2.$$

By a Taylor expansion around $\|u_{\max}\|^2 = 0$, we have:

$$= - \left(\|u_{\max}\|^2 + 6(\|u_{\max}\|^2)^2 + O((\|u_{\max}\|^2)^3) - \|u_{\max}\|^2 \right) \sum_{n=1}^{N} \hat{\varepsilon}_n^2.$$

By Assumptions 1 and 3, this is equal to $O(N^{-2p})O(N) = o(1)$.

Next we show that

$$\sum_{n=1}^{N} \left(\frac{1}{(1 - \|u_n\|^2)^3} - 1 \right) \left(1 - \|u_n\|^2 \right) \hat{\varepsilon}_n \langle u_n, \hat{\theta} \rangle = o(1).$$

To start, note that $\sum_n \hat{\varepsilon}_n \langle u_n, \hat{\theta} \rangle = \hat{E}^T U^T \hat{\theta} = 0$. We can then apply Lemma 3 to upper bound the absolute value of our quantity of interest:

$$\left| \sum_{n=1}^{N} \left(\frac{1}{(1 - \|u_n\|^2)^3} - 1 \right) \left(1 - \|u_n\|^2 \right) \hat{\varepsilon}_n \langle u_n, \hat{\theta} \rangle \right|$$

$$\leq \left(\frac{1}{(1 - \|u_{\max}\|^2)^3} - 1 \right) (1 - \|u_{\max}\|^2) \sum_{n=1}^{N} |\hat{\varepsilon}_n \langle u_n, \hat{\theta} \rangle| \tag{40}$$

Now, by a Taylor expansion of the quantity outside the sum around $\|u_{\max}\|^2 = 0$

$$= \left(0 + 3\|u_{\max}\|^2 + O((\|u_{\max}\|^2)^2) \right) \sum_{n=1}^{N} |\hat{\varepsilon}_n \langle u_n, \hat{\theta} \rangle|. \tag{41}$$

Applying Cauchy Schwarz along with Assumption 3:

$$\leq O(N^{-p}) \left(\sum_{n=1}^{N} \hat{\varepsilon}_n^2 \right)^{1/2} \left(\sum_{n=1}^{N} \langle u_n, \hat{\theta} \rangle^2 \right)^{1/2} \tag{42}$$

Applying Assumption 1 and then Assumption 2:

$$= O(N^{-p})O(N^{1/2})\|\hat{\theta}\|^2 = o(1). \tag{43}$$

$\square$

Lemma 6. *Take Assumptions 1 to 3 and as in the proof of Lemma 2, define:*

$$\delta^{(2)}(\lambda) := \sum_{n=1}^{N} \left(\left(\frac{1 + \lambda}{1 + \lambda - \|u_n\|^2} \right)^4 - 1 \right) (a_n \lambda^2 + b_n \lambda + c_n), \tag{44}$$

where a_n, b_n, c_n are as defined in the proof of Lemma 2. Then, for $\lambda \in [0, c]$, where $c > 0$ is some constant in N, we have that $\delta^{(2)}(\lambda) = o(1)$.

Proof. First, we have:

$$\left(\frac{1 + \lambda}{1 + \lambda - \|u_n\|^2} \right)^4 - 1 \leq \left(\frac{1 + \lambda}{1 + \lambda - \|u_{\max}\|^2} \right)^4 - 1 \tag{45}$$

$$= \left(0 + 4\|u_{\max}\|^2 + O((\|u_{\max}\|^2)^2) \right) \tag{46}$$

$$= O(N^{-p}) \tag{47}$$

where the second equality holds by a Taylor expansion around $\|u_{\max}\|^2 = 0$, and the third equality holds by Assumption 3. Now, we can bound $\delta^{(2)}(\lambda)$ as:

$$\delta^{(2)}(\lambda) \leq O(N^{-p}) \sum_{n=1}^{N} |a_n \lambda^2 + b_n \lambda + c_n| \leq O(N^{-p}) \sum_{n=1}^{N} |a_n| + |b_n| + |c_n|, \tag{48}$$

where the second inequality is a result of $\lambda \leq c = O(1)$. We now bound the sums $\sum_n |a_n|$, $\sum_n |b_n|$, and $\sum_n |c_n|$ to complete the proof.

$$\sum_{n=1}^{N} |a_n| \leq \sum_{n=1}^{N} 2\|u_n\|^2 \hat{\varepsilon}_n^2 + (1 - \|u_n\|^2) \langle u_n, \hat{\theta} \rangle^2 \tag{49}$$

$$= O(N^{1-p}) + (1 - O(N^{-p})) \left\| \hat{\theta} \right\|^2 \tag{50}$$

$$= O(N^{1-p}), \tag{51}$$

where the first line holds by the definition of a_n, the next by Assumptions 1 and 3, and the third by Assumption 2. We continue to bound:

$$\sum_{n=1}^{N} |b_n| \tag{52}$$

$$\leq \sum_{n=1}^{N} 2(1 - \|u_n\|^2)^2 \langle u_n, \hat{\theta} \rangle^2 + 4\|u_n\|^2 \hat{\varepsilon}_n^2 + (2 + 4(\|u_n\|^2)^2 + 6\|u_n\|^2) |\hat{\varepsilon}_n \langle u_n, \hat{\theta} \rangle| \tag{53}$$

$$= (2 + O(N^{-p}) \left\| \hat{\theta} \right\|^2 + O(N^{1-p}) + (2 + O(N^{-p})) \left(\sum_{n=1}^{N} \hat{\varepsilon}_n^2 \right)^{1/2} \left(\sum_{n=1}^{N} \langle u_n, \hat{\theta} \rangle^2 \right)^{1/2} \tag{54}$$

$$= O(\sqrt{N}), \tag{55}$$

where the first line is by definition of b_n, the second is by Assumptions 1 and 3 and the Cauchy-Schwarz inequality, and the third is by Assumptions 1 and 2. We continue by bounding:

$$\sum_{n=1}^{N} |c_n| \tag{56}$$

$$\leq \sum_{n=1}^{N} (1 - \|u_n\|^2)^2 \langle u_n, \hat{\theta} \rangle^2 + 4\|u_n\|^2 \hat{\varepsilon}_n^2 + (2 + 3(\|u_n\|^2)^2 + 3\|u_n\|^2) |\hat{\varepsilon}_n \langle u_n, \hat{\theta} \rangle| \tag{57}$$

$$\leq \left\| \hat{\theta} \right\|^2 + O(N^{1-p}) + (2 + O(N^{-p}) \left(\sum_{n=1}^{N} \hat{\varepsilon}_n^2 \right)^{1/2} \left(\sum_{n=1}^{N} \langle u_n, \hat{\theta} \rangle^2 \right)^{1/2} \tag{58}$$

$$= O(\sqrt{N}), \tag{59}$$

where the line-by-line reasoning is the same as that of our bound on $\sum_n |b_n|$ above. Plugging our bounds into Eq. (48), we get that for all $\lambda \in [0, c]$, we have that $\delta^{(2)}(\lambda) \leq O(N^{-p}) O(\sqrt{N}) = o(1)$, as $p > 1/2$ by Assumption 3. $\qquad \square$

F   Proof of Corollary 1

We first state a theorem about the concentration of i.i.d. sub-Gaussian matrices. Let $s_D \leq \cdots \leq s_1$ be the singular values of X.

Theorem 2 (Theorem 4.6.1 from Vershynin [2018]). *Suppose that the x_n are independent sub-Gaussian isotropic random vectors with maximum sub-Gaussian constant K. Then for some constant $C > 0$ and any $t \geq 0$, the following holds with probability at least $1 - 2e^{-t^2}$:*

$$\sqrt{N} - CK^2(\sqrt{D} + t) \leq s_D \leq s_1 \leq \sqrt{N} + CK^2(\sqrt{D} + t). \tag{60}$$

We now restate and then prove Corollary 1.

Corollary 1. *Take Assumptions 3 and 4. Assume we have a well-specified linear model for some $\theta^* \in \mathbb{R}^D$; that is, $y_n = \langle x_n, \theta^* \rangle + \varepsilon_n$, where $\varepsilon_n \overset{i.i.d.}{\sim} \mathcal{N}(0, \sigma^2)$. If σ is sufficiently small, $\hat{\theta}$ is consistent for θ^*, and the entries of the covariate matrix x_{nd} are i.i.d. sub-Gaussian random variables, then $\mathcal{L}$ is quasiconvex with probability tending to 1 as $N \to \infty$.*

Proof. The idea is to show that our assumptions imply that Assumptions 1 and 2 hold, as well as that the spectrum of X becomes uniform with high probability. Our assumption that $\hat{\theta}$ is consistent for θ^* immediately implies that $\|\hat{\theta}\| = O(1)$. Next, as discussed after Assumption 1, we can stack the ε_n into a vector $E \in \mathbb{R}^N$. We then have that $\|E\|^2 \geq \|(I_N - UU^T)E\|^2 = \|\hat{E}\|^2 = \sum_n \hat{\varepsilon}_n^2$. As $\|E\|^2 = O(N)$ with probability tending towards 1 as $N \to \infty$, we have that Assumption 1 holds with probability tending towards 1 as $N \to \infty$.

Now, by Theorem 2 with $t = N^{1/3}$ (any t that goes to infinity with N but is $o(\sqrt{N})$ will work), we have that the singular values of X satisfy

$$\sqrt{N} - o(\sqrt{N}) \leq s_D \leq s_1 \leq \sqrt{N} + o(\sqrt{N}). \tag{61}$$

with probability at least $1 - o(1)$. By Proposition 2, the quasiconvexity of $\mathcal{L}$ is invariant to a scaling of the singular values; thus we can divide all singular values by $\sqrt{N}$ to get that all singular values lie in the interval $[1 - o(1), 1 + o(1)]$ with probability going to 1. Thus, for any neighborhood Δ of $\mathbf{1} \in \mathbb{R}^D$, the (normalized) singular values will eventually lie within Δ with arbitrariliy high probability. Thus all of the conditions of Theorem 1 are met, implying that $\mathcal{L}$ will be quasiconvex with probability tending towards 1 as $N \to \infty$.

$\square$

G   Generating zero-mean orthonormal matrices uniformly at random

In our experiments in Section 6, we draw $N \times D$ orthonormal matrices U with zero-mean columns from the uniform distribution over such matrices. To do so, we generate vectors $a_1, \ldots, a_D \in \mathbb{R}^D$ such that $a_{nd} \overset{i.i.d.}{\sim} \mathcal{N}(0, 1)$. We then use the Gram-Schmidt process to orthogonalize the vectors $\{\mathbf{1}, a_1, \ldots, a_D\}$; the second through $D + 1$th outputted vectors make up the columns of U. Notice this procedure requires $N < D$.

In our experiments surrounding Assumption 1, we need to generate vectors $R \in \mathbb{R}^N$ such that $U^T R = 0$ uniformly over such R's. To do so, we generate a vector $a \sim \mathcal{N}(0, I_N)$. We then compute $b = (I_N - UU^T)a$; setting $R = b/\|b\|$ yields the result.

Why is this uniform over all vectors in the null space of U? Recall that a is an isotropic random vector. It is well-known that this implies that $a/\|a\|$ is uniform over the unit sphere. As multiplication by $I_N - UU^T$ is an orthogonal projection, we have that $b = (I_N - UU^T)a$ is isotropic over the null space of U. Thus $b/\|b\|$ is uniform over the null-space of U. The same reasoning shows that the use of the Gram-Schmidt algorithm to generate orthonormal zero-column-mean matrices U is uniform over such matrices – we start with isotropic random vectors, Gram Schmidt applies orthogonal projections to each and then normalizes the results.

H   Replicating experiments with error bars

For each of the experiments in Fig. 3 (our experiments about the size of the neighborhood Δ and U's violating Assumption 3), we repeat the experiment five times to understand the random variability in each experiment. Fig. 8 shows the result. All plots are created exactly as in Fig. 3, except each dot is now an average over all five trials. Error bars are equal to two times the standard deviation across these five trials. We see that our conclusions from Fig. 3 still hold. In some cases, the error bars are so small that they are barely visible on the scale of these plots.
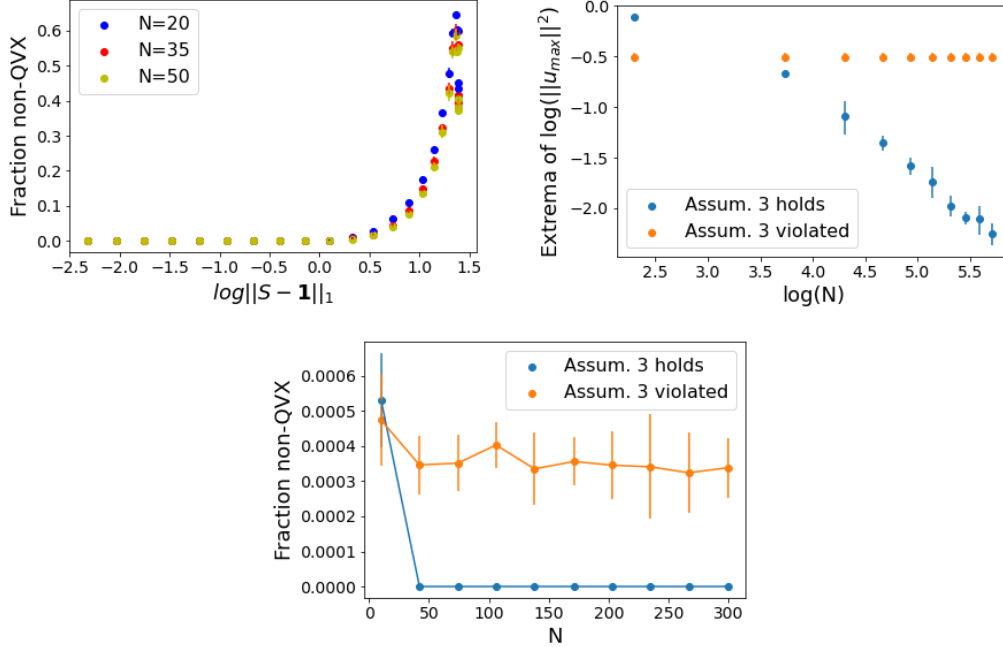
Figure 8: Replication of Fig. 3 with error bars; we repeat the original caption here for reading convenience. (*Upper left*): We generate many datasets and plot the fraction that are not quasiconvex, varying N and the distance of the spectrum from uniformity ($\|S - \mathbf{1}\|_1$). (*Upper right*): We generate two sets (orange, blue) of left-singular vector matrices U. In the blue case, we check that the maximum of $\log \|u_{\max}\|^2$ across all U for a particular N decreases roughly linearly on a log-log plot (i.e. the blue set satisfies Assumption 3). In the orange case, we check that the minimum of $\log \|u_{\max}\|^2$ across all U for a particular N is roughly constant (i.e. the orange set does not satisfy Assumption 3). (*Lower*): For all the U matrices from the upper right plot, we generate many datasets and plot the fraction that are not quasiconvex.

I   Implementation details of experiments

I.1   Efficiently computing $\mathcal{L}(\lambda)$

The LOOCV loss is given in Eq. (2) of the main text as:

$$\mathcal{L}(\lambda) := \sum_{n=1}^{N} \left(\langle x_n, \hat{\theta}^{\backslash n}(\lambda) \rangle - y_n \right)^2, \tag{62}$$

While this seems to require solving N regression problems to obtain $\hat{\theta}^{\backslash n}(\lambda)$ for $n = 1, \dots, N$, there is a well-known explicit formula for $\mathcal{L}$ that makes use of the Sherman-Morrison formula:

$$\mathcal{L}(\lambda) = \sum_{n=1}^{N} \frac{1}{(1 - Q_n)^2} \left(\langle x_n, \hat{\theta} \rangle - y_n \right)^2, \tag{63}$$

where $Q_n := x_n^T \left(X^T X + \lambda I_D \right)^{-1} x_n$.

Using the results of Proposition 2, we know that the matrix of right singular vectors V does not matter for the quasiconvexity of $\mathcal{L}$. So, in all of our experiments, we set $V = I_D$, which further simplifies Eq. (63). In particular, letting u_n be the nth row of U, we have $x_n = u_n \operatorname{diag}(S)$ and $Q_n = u_n^T \operatorname{diag}(S^2/(S^2 + \lambda)) u_n$. Then:

$$\mathcal{L}(\lambda) = \sum_{n=1}^{N} \frac{1}{\left(1 - u_n^T \operatorname{diag}\left(\frac{S^2}{S^2 + \lambda} \right) u_n \right)^2} \left(u_n^T \operatorname{diag}\left(\frac{S^2}{S^2 + \lambda} \right) U^T Y - y_n \right)^2. \tag{64}$$

We are given U and S in all of our experiments, so this formula is much faster to compute than Eq. (63), as it requires no matrix inversions.

I.2 Numerically checking for quasiconvexity

To check for quasiconvexity in our experiments, we evaluate $\mathcal{L}$ on a dense, regularly spaced grid $\lambda_1, \ldots, \lambda_T$. In this appendix, we describe how, given $\mathcal{L}(\lambda_1), \ldots, \mathcal{L}(\lambda_T)$, we check whether $\mathcal{L}$ is quasiconvex. In short, we numerically check whether $\mathcal{L}'$ ever switches from positive to negative (the condition for a local maximum); note that this must occur inbetween any two local minima, so we do not have to count the number of local minima. To approximate the sign of $\mathcal{L}'$, we use $s_i := \text{Sign}(\mathcal{L}(\lambda_{i+1} - \mathcal{L}(\lambda_i)))$ for $i = 1, \ldots, T - 1$. We then report quasiconvexity if there exists any i for which $s_i = 1$ and $s_{i+1} = -1$; that is, if our approximation to the derivative changes from positive to negative.

Note there are two ways in which this procedure can fail. The first is that our grid of λ_t's may be insufficiently dense to capture non-quasiconvex behavior; however, in practice, we have never observed this to be an issue, as we have never found increasing the density of the grid of λ's to reveal extra local minima. The second issue is that non-quasiconvex behavior may occur beyond the maximal λ_T we specify. We again do not have an exact way of preventing this in practice. However, in all of our experiments, we specify a λ_T that is orders of magnitude larger than the maximal singular value of X. At this point, we expect $\mathcal{L}(\lambda)$ to be an essentially flat function; thus, any missed local minima are likely of effectively the same value as $\mathcal{L}(\infty)$. In any case, if either failure mode were occurring in our of our experiments, fixing it would only make the (already concerning) non-quasiconvexity in our experiments look more severe.